

The female-specific Doublesex isoform regulates pleiotropic transcription factors to pattern genital development in *Drosophila*

Sujash S. Chatterjee, Locke D. Uppendahl*, Moinuddin A. Chowdhury, Pui-Leng Ip and Mark L. Siegal†

SUMMARY

Regulatory networks driving morphogenesis of animal genitalia must integrate sexual identity and positional information. Although the genetic hierarchy that controls somatic sexual identity in the fly *Drosophila melanogaster* is well understood, there are very few cases in which the mechanism by which it controls tissue-specific gene activity is known. In flies, the sex-determination hierarchy terminates in the *doublesex* (*dsx*) gene, which produces sex-specific transcription factors via alternative splicing of its transcripts. To identify sex-specifically expressed genes downstream of *dsx* that drive the sexually dimorphic development of the genitalia, we performed genome-wide transcriptional profiling of dissected genital imaginal discs of each sex at three time points during early morphogenesis. Using a stringent statistical threshold, we identified 23 genes that have sex-differential transcript levels at all three time points, of which 13 encode transcription factors, a significant enrichment. We focus here on three sex-specifically expressed transcription factors encoded by *lozenge* (*lz*), *Drop* (*dr*) and *AP-2*. We show that, in female genital discs, *Dsx* activates *lz* and represses *dr* and *AP-2*. We further show that the regulation of *dr* by *Dsx* mediates the previously identified expression of the fibroblast growth factor *Branchless* in male genital discs. The phenotypes we observe upon loss of *lz* or *dr* function in genital discs explain the presence or absence of particular structures in *dsx* mutant flies and thereby clarify previously puzzling observations. Our time course of expression data also lays the foundation for elucidating the regulatory networks downstream of the sex-specifically deployed transcription factors.

KEY WORDS: Sexual differentiation, Genitalia, Pattern formation, *Drosophila*

INTRODUCTION

Many aspects of animal physiology, behavior and body structure show differences between the sexes. The most obvious sexual dimorphism is in the reproductive organs. Much is known about the genetic control of sex-determination in model and non-model organisms (Cline and Meyer, 1996; Marín and Baker, 1998; Manolakou et al., 2006), yet relatively little is known about the mechanisms that integrate sexual identity and positional cues to control genital morphogenesis (Christiansen et al., 2002; Estrada et al., 2003).

The sex-determination hierarchy of *Drosophila melanogaster* has three branches that respectively control X-chromosome dosage compensation, male courtship behavior and most somatic sexual differentiation (Christiansen et al., 2002). In the third branch, alternative splicing of *doublesex* (*dsx*) pre-mRNA produces sex-specific transcription factors with identical DNA-binding domains. The canonical example of how *Dsx* regulates its targets is provided by the yolk protein genes *Yp1* and *Yp2*, which share an enhancer to which *Dsx* binds (Burtis et al., 1991). The female isoform (*DsxF*) activates, whereas the male isoform (*DsxE*) represses, *Yp* gene expression (Bownes, 1994). Similar effects of *DsxF* and *DsxE* are seen at an enhancer of the tandem *bric à brac 1* (*bab1*) and *bab2*

genes, which control abdominal pigmentation (Kopp et al., 2000; Williams et al., 2008). *Dsx* also binds to an enhancer of *Fad2*, which is involved in producing female pheromones (Shirangi et al., 2009). *DsxF* is required for activating *Fad2*, but *DsxE* is not required for its repression in males (Shirangi et al., 2009).

The *Yp1/2*, *bab1/2* and *Fad2* enhancers are the only known direct targets of *Dsx*. Efforts to find other targets have included microarray studies profiling transcriptomes of males, females and sex-determination mutants. Whole adult flies (Arbeitman et al., 2004), whole pupae (Lebo et al., 2009) and adult heads and central nervous systems (Goldman and Arbeitman, 2007) have been assayed. From these studies, regulation by *Dsx* appears to be more complex than the direct target examples suggest, in that any given gene might be activated or repressed by *DsxF* and activated or repressed by *DsxE*. However, as these studies acknowledged, the apparent complexity might result from indirect interactions.

Although no known case of direct regulation by *Dsx* occurs in genital tissue, it is likely that the developing genitalia are a major site of *Dsx* action. Indeed, whereas many cells do not even ‘know’ their sex, as defined by expression of *dsx* (Hempel and Oliver, 2007; Camara et al., 2008; Arbeitman et al., 2010; Robinett et al., 2010), nearly every cell of the developing genitalia expresses *dsx* at the onset of metamorphosis (Robinett et al., 2010). The genitalia derive from the genital imaginal disc (Nöthiger et al., 1977; Schüpbach et al., 1978; Cohen, 1993), which is patterned during larval life and differentiates into the terminalia (genitalia and analia) during metamorphosis (Fig. 1). Abdominal segments A8, A9 and A10 contribute cells to the disc. The female genitalia derive predominantly from the A8 primordium, the male genitalia predominantly from the A9 primordium, and the analia from the A10 primordium (Christiansen et al., 2002; Estrada et al., 2003).

Center for Genomics and Systems Biology, Department of Biology, New York University, New York, NY 10003, USA.

*Present address: School of Medicine, University of Kansas, Mail Stop 1049, 3901 Rainbow Boulevard, Kansas City, KS 66160, USA

†Author for correspondence (mark.siegel@nyu.edu)

Two genes that are expressed sex-differentially in the genital disc, *branchless* (*btl*) and *dachshund* (*dac*), provide our best picture of how *dsx* controls genital morphogenesis. *Btl*, which is the fly fibroblast growth factor (FGF), is expressed in two bowl-like sets of cells in the A9 primordium in male discs; there is no expression in female discs because *Dsx*F cell-autonomously represses *btl* (Ahmad and Baker, 2002). *Btl* recruits mesodermal cells expressing the FGF receptor Breathless (Btl) to fill the bowls; these Btl-expressing cells develop into the vas deferens and accessory glands (Ahmad and Baker, 2002).

Dac, a transcription factor, is expressed in male discs in lateral domains of the A9 primordium and in female discs in a medial domain of the A8 primordium (Keisman and Baker, 2001). These lateral and medial domains correspond to regions exposed to high levels of the morphogens Decapentaplegic (Dpp) and Wingless (Wg), respectively. *Dsx* determines whether these signals activate or repress *dac* (Keisman and Baker, 2001). Male *dac* mutants have small claspers with fewer bristles and lack the single, long mechanosensory bristle (Gorfinkiel et al., 1999; Keisman and Baker, 2001). Female *dac* mutants have fused spermathecal ducts (Keisman and Baker, 2001) and a disorganized gonopod (Gorfinkiel et al., 1999).

To identify more genes that are expressed sex-differentially in the developing genitalia, and in particular to find genes with major patterning roles during genital morphogenesis, we transcriptionally profiled male and female genital discs at three time points. Because key patterning genes are expressed in late third-instar larval (L3) genital discs (Chen and Baker, 1997; Gorfinkiel et al., 1999; Keisman and Baker, 2001; Keisman et al., 2001; Ahmad and Baker, 2002), our first time point is L3. Our next time points, at ~6 (P6) and 20 (P20) hours after puparium formation (APF), are times of important morphogenetic change (Fig. 1I-L). In P6 male discs, Btl-expressing cells begin transitioning to epithelium as they differentiate into the vas deferens and accessory glands (Ahmad and Baker, 2002). By P20, this transition is complete (Ahmad and Baker, 2002); a clear division between internal and external terminalia is also evident (P. Ehrenspurger, Diplomarbeit, University of Zürich, 1972). In P6 female discs, the ducts of the accessory glands and spermathecae emerge as protuberances of the disc epithelium. At P20, each protuberance has formed a lumen and the ducts begin elongating out of the disc; a clear division between internal and external terminalia is also evident (Epper, 1983).

Our microarray results provide a global profile of early genital morphogenesis. They also led us to focus on three genes – *lozenge* (*lz*), *Drop* (*dr*) and *AP-2* – that are sex-specifically expressed at all three time points assayed and that encode well-studied transcription factors. *Lz* functions in eye and blood cell development (Canon and Banerjee, 2000). *Dr* [also known as Muscle segment homeobox (Msh)], functions in muscle development (Furlong, 2004), neural development (Ramos and Robert, 2005) and dorsal fate specification (Milán et al., 2001). *AP-2* functions in limb outgrowth and brain development (Monge et al., 2001). We show how *Dsx* limits the expression of each of these factors to the genital disc of one sex, and how these factors contribute to genital morphogenesis.

MATERIALS AND METHODS

Fly strains and crosses

Flies were raised on standard medium and, unless specified otherwise, at 25°C. Alleles and chromosomes are described in FlyBase (Tweedie et al., 2009). Genital discs for microarrays and *in situ* hybridizations were dissected from *esg*^{GAL4,B}, *UAS-GFPnls/CyO* and Canton-S flies, respectively. Three stocks containing *dsx*-null mutations were used: (1) *w*;

Df(3R)dsx15/TM6B, *Tb*, which carries a large deficiency spanning *dsx*; (2) *w*; *Df(3R)f01649-d09625/TM6B*, *Tb*; and (3) *w*; *Df(3R)f00683-d07058/TM6B*, *Tb*. The latter two deficiencies are FLP/FRT-mediated deletions that eliminate all *dsx* coding sequence but leave neighboring genes intact. These deletions, the endpoints of which are piggyBac insertions corresponding to the designations following ‘*Df(3R)*’ (Parks et al., 2004), were generated and generously provided before publication by Carmen Robinett (Janelia Farm Research Campus, Howard Hughes Medical Institute, VA, USA). We confirmed the extents of these deletions, and the absence of *dsx* sequences in *Df(3R)dsx15*, by PCR analysis of genomic DNA.

For RNAi, the *NP6333-Gal4* driver (*P{GawB}Pen^{NP6333}*), which expresses in wing, leg and genital discs (Stieper et al., 2008), was used. Gene-specific *UAS-RNAi* constructs were obtained from the Vienna *Drosophila* RNAi Center, and the *UAS-Dicer-2* transgene *P{UAS-Dcr-2.D}* was used to increase RNAi activity (Dietzl et al., 2007).

Ectopic expression clones were generated using flip-out Gal4 (Ito et al., 1997; Pignoni and Zipursky, 1997) by heat shocking first-instar larvae (24–48 hours after egg laying) at 38°C. GFP-labeled feminized clones were generated in *y w*, *P{hsFLP}1/Y*; *P{AyGAL4}P{UAS-tra.F}*; *P{UAS-GFP.S65T}+/+* larvae. *P{AyGAL4}* expresses Gal4 under the control of the *Actin 5C* promoter only after FLP excises an intervening *y⁺* cassette. Heat-shocked larvae were incubated at 18°C until dissection at L3 [following Keisman and Baker (Keisman and Baker, 2001)]. Masculinized clones were generated by heat shocking *w*, *P{UAS-tra2.IR}61X/w*, *P{hsFLP}1/+P{AyGAL4}*; *P{UAS-tra2.IR}82A-3/P{UAS-GFP.S65T}* larvae. *Dr* loss-of-function clones were generated by heat shocking *y w*, *P{hsFLP}1/Y*; *P{AyGAL4}*, *P{UAS-GFP.S65T}+/+*; *UAS-DrRNAi*, *UAS-Dcr-2/bnl-lacZ* larvae. The *bnl-lacZ* insertion is the enhancer-trap allele *bnl⁰⁶⁹¹⁶*.

L3 expression of *eyg* and *ap* and pupal expression of *lz* were assayed using the enhancer-trap alleles *eyg^{M3-12}*, *ap^{rK568}* and *lz^{gal4}*, respectively.

Morphological staging and dissections

Wandering L3 larvae were sexed by gonad size. Collections from pupal stages were standardized using sex-nonspecific morphological landmarks (Bainbridge and Bownes, 1981). Each sex-sorted larva was observed until it reached the white prepupa stage (0 hours APF), which lasts 15–20 minutes and thereby improves synchronization of the following stages. An air bubble forms mid-dorsally on the puparium at ~4 hours APF and peaks in size at 6–6.5 hours APF. For P6 samples, rather than merely timing 6 hours since white prepupa, each animal was observed every 20 minutes from 5 hours APF until peak bubble size was evident, at which time its genital disc was dissected. For P20, we observed that *esg*-driven GFP expression in an oval patch in the eye disc becomes visible at ~20 hours APF. We observed each pupa every 20 minutes from 18 hours APF until GFP appeared in the eye, at which time its genital disc was dissected. Morphologies of P6 and P20 discs collected this way showed little within-sex variation and matched previous descriptions (P. Ehrenspurger, Diplomarbeit, University of Zürich, 1972) (Epper, 1983).

RNA isolation and microarray analysis

For each microarray sample, about ten L3, five P6 or five P20 discs were dissected in cold PBS and immediately transferred into Ambion MELT lysis buffer. Total RNA was extracted, then purified and concentrated using Qiagen RNeasy MinElute. RNA integrity and concentration were determined by Bioanalyzer (Agilent, Santa Clara, CA, USA) and NanoDrop ND-1000A (Thermo Fisher Scientific, Waltham, MA, USA). From 20 ng RNA per sample, biotin-labeled cDNA was produced by linear amplification with the NuGEN Ovation Biotin System. cDNA was quantified by NanoDrop and 1.5 µg hybridized to an Affymetrix GeneChip *Drosophila* Genome 2.0 Array and scanned following the manufacturer’s protocols. Analyses were performed using R/Bioconductor (Gentleman et al., 2004). Microarray data are deposited in NCBI GEO with accession GSE23344.

In situ hybridizations

In situ hybridizations used digoxigenin-labeled antisense riboprobes (Sullivan et al., 2000; Kosman et al., 2004). Probe templates were either linearized cDNA clones (*Drosophila* Genomics Resource Center) or PCR-amplified sequences (clone IDs and PCR primer sequences are listed in Table S1 in the supplementary material).

Immunofluorescence

Larval tissues were dissected in cold PBS, fixed in 4% paraformaldehyde for 45 minutes, washed in PBS containing 0.2% Triton X-100 and incubated with primary antibodies at 4°C overnight (Xu and Rubin, 1993). Primary antibodies were mouse anti-Lz (1:10 dilution; Developmental Studies Hybridoma Bank), rat anti-Al (1:100) (Campbell et al., 1993), rabbit anti-Dr (1:500) (von Ohlen and Doe, 2000), rabbit anti-AP-2 (1:1000) (Monge et al., 2001) and rabbit anti- β -gal (1:500; Promega). Alexa Fluor-conjugated secondary antibodies were used (1:1000; Invitrogen). Discs were mounted in DAPI-containing Vectashield. Confocal images were acquired using a Leica SP5 scanning microscope.

Dsx binding site analysis

All matches to the ACAATGT Dsx consensus binding sequence within non-coding sequence were identified using Target Explorer (Sosinsky et al., 2003). Sequence coordinates of each gene were obtained from FlyBase R5.29 (Tweedie et al., 2009).

RESULTS

Genome-wide profiling identifies transcripts expressed differentially in developing male and female genital discs

To identify genes involved in sex-specific differentiation of the genitalia, we transcriptionally profiled male and female genital discs at three time points: L3, P6 and P20 (see Materials and methods; Fig. 1). To aid in identifying genital discs, and thereby avoid loss or contamination of tissue, we used animals expressing GFP in all imaginal discs (*esg*^{GAL4,B}, *UAS-GFP.nls/CyO*) (Keisman et al., 2001). Four biological replicates were performed for each sex at each time point. Affymetrix GeneChip data were background corrected and normalized using RMA (Irizarry et al., 2003) and sex-differential expression was tested using significance analysis of microarrays (SAM), which controls the false discovery rate (FDR) (Tusher et al., 2001).

We validated microarray accuracy by verifying that all previously identified sex-differentially expressed genes were identified as such in our analysis, and by visualizing the expression of a representative subset of previously uncharacterized genes in genital discs. Five loci were previously shown to be expressed sex-differentially in L3 genital discs. Of these, all five were significantly differentially expressed in our analysis at a stringent FDR threshold of 0.05: *btl* and *btl* (Ahmad and Baker, 2002); *abdominal A* (*abd-A*) (Freeland and Kuhn, 1996; Casares et al., 1997; Chen et al., 2005); *Wnt oncogene analog 2* (*Wnt2*) (Kozopas et al., 1998); and the paralogous, adjacent *spalt* (*sal*) genes (Dong et al., 2003). Additional significant loci can be considered positive controls as well, although their expression in genital discs had not been quantified directly: the female-specific *dsx* isoform; *male-specific lethal 2* (*msl-2*), which shows lower mRNA levels in whole females than males (Bashaw and Baker, 1997); *babI/2*, the protein expression of which in L3 discs appears different in males and females but had not been quantified (Couderc et al., 2002); *Pox neuro* (*Poxn*), which was shown to be expressed in male discs at time points later than ours (Boll and Noll, 2002); and *stumps*, which appears upregulated in *btl*-expressing cells as they transition to epithelium (Ahmad and Baker, 2002) and which shows, consistent with this observation, significantly male-biased expression at P6 and P20 but not L3. Another notable gene is *paired* (*prd*), which is required for male accessory gland development but was undefined in terms of genital disc expression (Xue and Noll, 2002). We find *prd* expression significantly male biased at P6 and P20. A final gene that can be considered a positive control is *Myosin 31DF* (*Myo31DF*), which controls directional

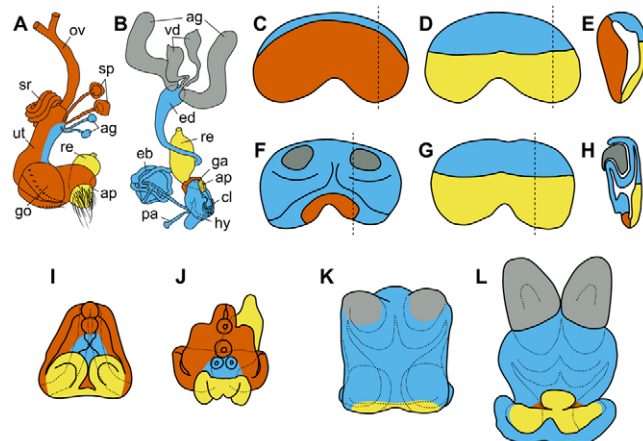


Fig. 1. The terminalia of *D. melanogaster* and their development from an imaginal disc. Adult female (A) and male (B) derivatives of the genital disc. The genital disc of a late third-instar female (C-E) or male (F-H) larva is shown in ventral view, dorsal view and parasagittal section, respectively. Parasagittal-section positions are shown as dashed lines (C,D,F,G). The female (I,J) or male (K,L) genital disc is shown in dorsal view 6 or 20 hours after puparium formation (APF), respectively. Derivatives of embryonic segment A8 are in orange, A9 in blue and A10 in yellow. Derivatives of recruited mesodermal cells are in gray. ov, oviduct; sp, spermathecae; sr, seminal receptacle; ut, uterus; ag, accessory gland; re, rectum; go, female gonopod; ap, anal plates; vd, vas deferens; ed, ejaculatory duct; eb, ejaculatory bulb; ga, genital arch; cl, claspers; pa, penis apodeme; hy, hypandrium. Schematics in A,B are adapted from Bryant (Bryant, 1978) and Keisman et al. (Keisman et al., 2001) with kind permission from Elsevier, those in I,J are adapted from Epper (Epper, 1983) with kind permission from Springer Sciences+Business Media and those in K,L are adapted with kind permission of P. Ehrenspäßer (P. Ehrenspäßer, Diplomarbeit, University of Zürich, 1972).

rotation of the male disc during metamorphosis (Spéder et al., 2006). *Myo31DF* has been shown to be expressed in the male genital disc at L3 (Spéder et al., 2006) and at 25 hours APF when rotation commences (Suzanne et al., 2010), although it has not been reported whether *Myo31DF* is sex-specifically transcribed. We find *Myo31DF* to be male biased at all three time points, but significantly so only at P20.

Our validation of previously uncharacterized genes focused on L3. SAM identified 55 probe sets (corresponding to 51 unique, annotated genes) with sex-differential L3 expression at a FDR threshold of 0.05 (see Table S2 in the supplementary material). We assayed genital disc expression of 17 of these genes by in situ hybridization and, when possible, using enhancer traps or immunofluorescence. As shown below and in Fig. S1 in the supplementary material, all 17 showed sex-differential expression in L3 genital discs, strongly validating the microarray analysis.

Having gained confidence in our microarray results, we proceeded with analysis of the P6 and P20 data. The number of genes with significant sex-differential expression increases through development: at the identical FDR threshold of 0.05, SAM identified sex-differential expression for 319 probe sets (297 genes) at P6 (see Table S3 in the supplementary material) and 435 probe sets (400 genes) at P20 (see Table S4 in the supplementary material). This increase through development is perhaps expected, as male and female tissues become ever more divergent from one another.

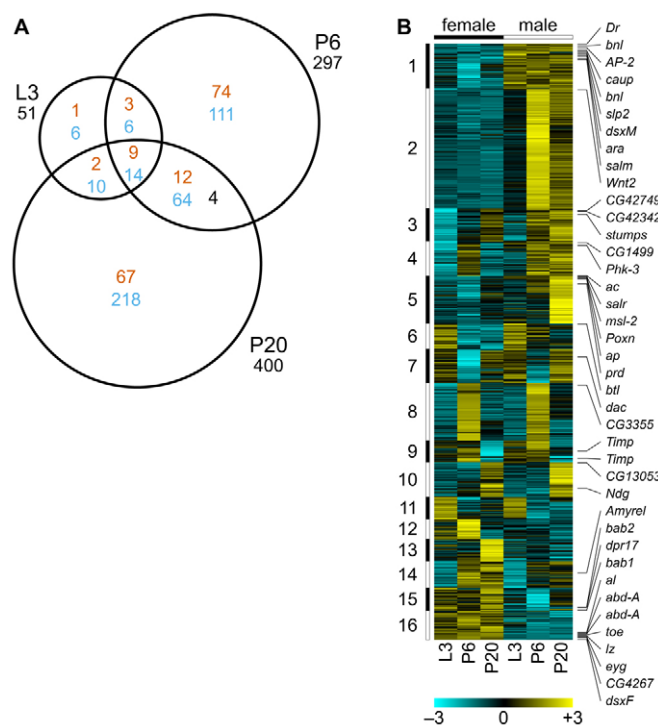


Fig. 2. Genes expressed sex-differentially in *Drosophila* genital discs. (A) Venn diagram summarizing transcriptional profiling comparisons at late third instar (L3) and 6 (P6) or 20 (P20) hours APF. The numbers of genes that were expressed significantly more highly in female discs are in orange and those expressed significantly more highly in male discs are in blue [the four remaining genes (black) switch sex bias from P6 to P20]. (B) PAM-clustered heat map of expression values of significantly sex-differentially expressed probe sets. Values are median-centered by probe set (row) and on a log₂ scale, as indicated. Genes and cluster numbers discussed in the text are indicated.

In total, 601 genes show significant sex-differential expression for at least one time point (Fig. 2A). Of these, 124 are significant at two or more time points. Of the 124, only four – *achaete* (*ac*), *Tissue inhibitor of metalloproteases* (*Timp*), *Nidogen/entactin* (*Ndg*) and *Amyrel* – switch sex bias. All four show significantly higher expression in females at P6 and in males at P20. That the vast majority of differentially expressed genes show consistent sex bias across time points suggests that, during early morphogenesis, male and female discs consistently differ either in the relative importance of the processes in which these genes participate or in the relative proportion of tissue undergoing these processes. The switch in expression of the four exceptions could reflect sex differences in the timing of particular processes. The proneural gene *ac* shows dynamic expression in wing discs (Skeath and Carroll, 1991). The male and female genitalia might differ in the dynamics of sensory organ specification. Likewise, *Timp* is involved in tissue remodeling during wing morphogenesis (Kiger et al., 2007) and *Ndg* encodes an extracellular matrix protein (Artero et al., 2003). Male and female discs might perform similar remodeling steps at different times. *Amyrel* encodes an amylase (Da Lage et al., 1998), the potential role of which in morphogenesis is unclear.

Although few genes switch sex-differential expression across developmental stages, clustering of transcriptional profiles for the 601 significant genes does reveal distinct expression patterns (Fig.

2B). The gene expression profiles were divided into 16 clusters (see Table S5 in the supplementary material) using partitioning around medoids (PAM) (Kaufman and Rousseeuw, 1990) with an average-silhouette strategy to choose the appropriate number of clusters (van der Laan et al., 2003). To explore the biological significance of these clusters, we tested for over-representation of gene ontology (GO) molecular function annotations within clusters. At top and bottom of the clustergram (clusters 1 and 16) are genes with higher expression in males or females, respectively, at all three time points. In both clusters, several related terms associated with transcription factors are over-represented (the most over-represented term for cluster 1 is ‘transcription regulator activity’, $P=9.1\times 10^{-7}$, Bonferroni-corrected hypergeometric test; for cluster 16 ‘transcription factor activity’, $P=8.7\times 10^{-6}$). Because such sex-differentially expressed regulatory genes are prime candidates for driving sex-specific genital development, we focused on these genes for subsequent analyses, as described below.

Three other clusters are also over-represented with transcriptional regulators: cluster 4, which contains genes highly expressed in females and males at P6, but in males only at P20 (‘transcription factor activity’, $P=0.018$); cluster 5, which contains genes highly expressed in males at P20 (‘specific RNA polymerase II transcription factor activity’, $P=0.0011$); and cluster 15, which like cluster 16 contains genes highly expressed in females at all three time points, although with a dip in both sexes at P6 (‘transcription factor activity’, $P=0.00035$). Two clusters have other over-represented functions. Cluster 2, which contains genes highly expressed in males at P6 and P20, is over-represented with metalloexopeptidases ($P=0.00068$). All five metalloexopeptidases in this cluster are abundant in the adult *vas deferens* (Dorus et al., 2006; Takemori and Yamamoto, 2009). Cluster 13, which contains genes highly expressed in females at P20, is over-represented with genes encoding structural constituents of the chitin-based cuticle ($P=0.029$). This result could mean that females and males deposit cuticle at different times, and supports the previous finding that cuticle-related genes show sex-differential expression during metamorphosis (Lebo et al., 2009).

Enrichment of Dsx binding sites in sex-differentially expressed genes

To determine whether the set of significantly sex-differentially expressed genes is likely to contain direct Dsx targets, we tested for enrichment of putative Dsx binding sites. In vitro selection of Dsx-binding oligonucleotides (Erdman et al., 1996), as well as footprinting analyses of Dsx direct targets (Burtis et al., 1991; Williams et al., 2008; Shirangi et al., 2009), point to the 7-mer ACAATGT as a strong consensus Dsx binding site. Because *Drosophila* enhancers may reside distant from the transcriptional start site, including in introns, we searched for ACAATGT matches within different distances (0.5, 1, 2, 5 or 10 kb) from the annotated beginning of each gene, with any match within an intron or untranslated region (UTR) considered to be at 0 distance. For each distance cut-off, there are significantly more ACAATGT matches among the sex-differentially expressed genes than among the remainder; this result holds for genes differentially expressed at L3, P6 or P20, as well as for the union of these gene sets (see Table S6 in the supplementary material). The sex-differentially expressed genes have larger introns on average, but this difference does not negate the over-representation of putative Dsx sites, as comparisons based on the density, rather than the number, of sites are significant as well (see Table S7 in the supplementary material). The largest over-representation of putative Dsx sites occurs for L3 (e.g. for the

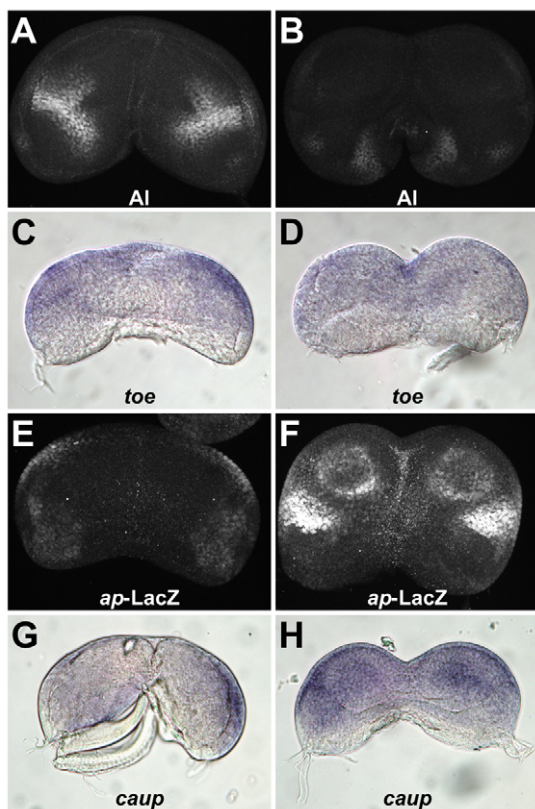


Fig. 3. Sex-differential expression of genes encoding transcription factors. (A–H) Female (A,C,E,G) and male (B,D,F,H) *Drosophila* genital discs. (A,B) Anti-Al immunofluorescence. (C,D) In situ hybridization with *toe* mRNA. Its paralog *eyg* is expressed in a matching pattern, as visualized with *eyg-lacZ* (not shown). (E,F) Anti- β -gal immunofluorescence of the *ap-lacZ* enhancer trap (which matches the *ap* mRNA expression pattern, not shown). (G,H) In situ hybridization with *caup* mRNA. Immunofluorescence images are maximum intensity confocal projections.

0.5 kb distance, there are 2.76-fold more ACAATGT matches for the sex-differentially expressed genes at L3, 1.55-fold more at P6 and 1.47-fold more at P20). Sex-differential expression at later time points might therefore be due to more indirect regulation.

Sex-differentially expressed transcription factors as candidate regulators of sex-specific genital morphogenesis

Twenty-five probe sets (23 genes) have significant male-biased or female-biased expression at all three time points (Fig. 2A). Of these genes, 13 are annotated with ‘transcription factor activity’, a highly significant enrichment ($P=1.56\times 10^{-10}$). These 13 include the positive-control genes *abd-A*, *salr*, *dsx*, *bab1* and *Poxn*. The remaining eight with previously uncharacterized sex-differential expression are *aristaleless* (*al*), *eyegone* (*eyg*), *twin of eyg* (*toe*), *lz*, *apterous* (*ap*), *caupolican* (*caup*), *Dr* and *AP-2*.

Five of the eight genes show expression in both female and male genital discs, but, consistent with the microarrays, expression is clearly higher in one sex (Fig. 3). Three (*al*, *eyg* and *toe*) are female biased. The *eyg* and *toe* genes are paralogs expressed in nearly identical domains in other tissues (Yao et al., 2008). The others (*ap* and *caup*) are male biased. Further characterization of *al*, *eyg/toe*, *ap* and *caup* will be presented elsewhere.

The remaining three of the eight genes are expressed exclusively in female (*lz*) or male (*Dr*, *AP-2*) discs. Through genetic and clonal analysis, we characterized their positions in the sexual-differentiation hierarchy and their roles in genital morphogenesis.

DsxF activates *lz* to promote development of the spermathecae and female accessory glands

In L3 female discs, *lz* is expressed in an anterior medial domain in the A8 primordium and in lateral domains in the A9 primordium (Fig. 4A). In male discs, *lz* is not expressed (Fig. 4B). During metamorphosis, *lz* is expressed in the primordia of the spermathecae and accessory glands as they form ducts that grow out of the female disc (Fig. 4C–E). Anderson (Anderson, 1945) showed that female *lz* mutants lack spermathecae and accessory glands. Using a temperature-sensitive allele we confirmed this result and showed that, consistent with its continued expression throughout metamorphosis, *lz* continues to be required after L3 for proper differentiation of these organs (Fig. 4F–H). Females homozygous for *lz*^{ts1} were raised at 16°C, the permissive temperature, then shifted to 29°C, the restrictive temperature. When the shift occurred at L3, spermathecae and accessory glands completely failed to form (Fig. 4G). When the shift occurred at ~P24 (a developmental stage equivalent to ~24 hours APF at 25°C), spermathecal ducts formed but often at least one of the spermathecal caps was absent (Fig. 4H).

To determine if and how *dsx* regulates *lz* in the genital disc, we examined *Lz* expression in *dsx*-null flies [*Df(3R)f00683-d07058/Df(3R)f01649-d09625*]. We observed a complete absence of *Lz* (Fig. 4I). Thus, DsxF is required to activate *lz* in female genital discs. This requirement is cell-autonomous. When a GFP-marked masculinized clone [expressing RNAi against *transformer* 2 and therefore expressing DsxM rather than DsxF (Fortier and Belote, 2000)] intersected the normal *lz* expression domain, *Lz* expression was lost (Fig. 4J). To test whether DsxF is sufficient to activate *lz* expression in the male disc, we assayed feminized clones expressing the female isoform of the *dsx* splicing regulator Transformer (Tra) (Ferveur et al., 1995). We examined 24 male discs with Tra-expressing clones. In two of the discs we observed ectopic *Lz*. *Lz* expression was confined to cells within a clone, implying cell-autonomous activation, but not all cells within the clone expressed *Lz*, suggesting that DsxF functions with one or more spatially restricted factors to activate *lz* (Fig. 4K). Consistent with spatially restricted competence to activate *lz* in response to DsxF, we did not observe ectopic *Lz* expression in the remaining 22 clone-bearing discs.

Because *dsx*-null discs lack *lz* expression and because *lz* is required for development of spermathecae and female accessory glands, *dsx*-null flies should lack these organs. However, previous studies observed these organs in the putatively null mutants *dsx*¹ (Hildreth, 1965) and *Df(3R)dsx15/dsx23* (Arbeitman et al., 2004), with one or two spermathecae found in 24% of mutant animals (Hildreth, 1965). Because of this discrepancy, we re-examined the presence of spermathecae and female accessory glands in unambiguously *dsx*-null flies. Out of 50 *Df(3R)f00683-d07058/Df(3R)f01649-d09625* and 50 *Df(3R)f00683-d07058/Df(3R)dsx15* animals, none had spermathecae or female accessory glands. Therefore, the true loss-of-function phenotype for *dsx* is an absence of spermathecae and female accessory glands, as reflected in the loss of *lz* expression in *dsx* mutant genital discs.

DsxF represses *Dr* in the female genital disc

Dr is expressed exclusively in male discs, in two domains (Fig. 5A,B): (1) a medial domain on the ventral surface of the A9 primordium encompassing the *bnl*-expressing cells but extending

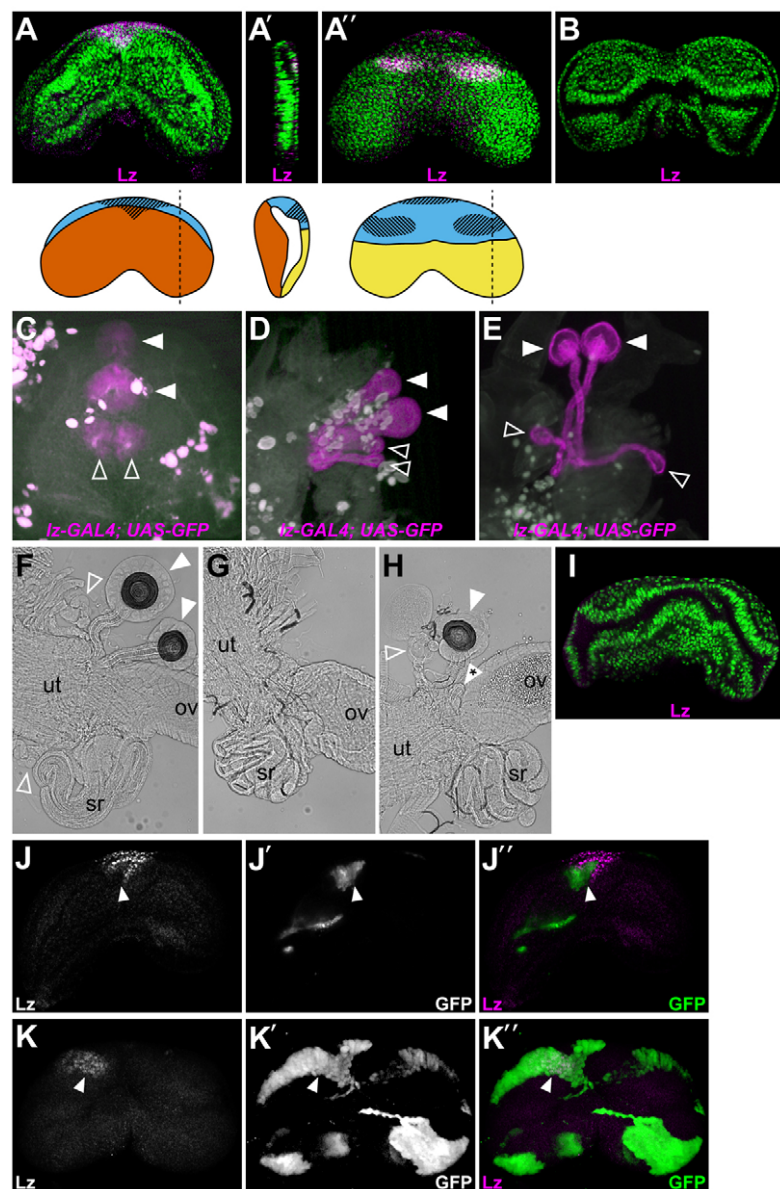


Fig. 4. Sex-specific expression, function and regulation of *Lz*. (A,B) Anti-Lz immunofluorescence (magenta). Shown are a confocal slice near the ventral face of the female disc (A), a reconstructed parasagittal section (A') and a confocal slice near the dorsal face (A''). Ventral, parasagittal and dorsal views are schematized beneath, with Lz expression indicated by the striped regions. Dashed lines indicate the approximate parasagittal section position. (B) Representative confocal slice toward the ventral surface of the male disc. (C-E) Expression of *Lz* in P20 (C), P38 (D) and P67 (E) female discs in the cells giving rise to the spermathecae (white arrowheads) and accessory glands (open arrowheads), as visualized by *Lz-Gal4*-driven GFP expression (magenta). (F-H) *Lz^{ts1}* female raised at the permissive temperature (F), or shifted to the restrictive temperature at L3 (G) or ~P24 (H). Arrowheads as in C-E; asterisk denotes spermathecal duct without cap. (I) Representative confocal slice toward the ventral surface of a *dsx*-null genital disc, showing the absence of Lz expression (magenta). (J-J'') Reduced Lz expression in a masculinized clone (arrowhead). Lz expression (J) and GFP-marked clones (J'') are shown individually, then merged in magenta and green, respectively (J''). (K-K'') Induced Lz expression in a feminized clone (arrowhead). Lz expression (K) and GFP-marked clones (K'') are shown individually, then merged in magenta and green, respectively (K''). Nuclei in A,B,I are counterstained with DAPI (green). Abbreviations as in Fig. 1.

laterally and posteriorly; and (2) a subset of the *btl*-expressing cells that are adjacent to those expressing *bnl* (and *Dr*). To determine if and how *dsx* regulates *Dr* in the genital disc, we assayed *Df(3R)f00683-d07058/Df(3R)f01649-d09625* animals. *Dr* is expressed in the A9 primordium of *dsx*-null discs (Fig. 5C), implying that DsxM is not required for *Dr* expression and instead that DsxF represses *Dr* in female discs. *Dr* repression by DsxF is cell-autonomous. When GFP-marked feminized clones in male discs intersected the normal *Dr* expression domain, *Dr* expression was lost (Fig. 5D).

***Dr* is required to activate *bnl* expression in the male genital disc**

Because *Dr* is expressed in the *bnl*-expressing cells, and because DsxF represses both *bnl* (Ahmad and Baker, 2002) and *Dr* (this study), we hypothesized that *Dr* is required to activate *bnl* in the male disc. To test this, we reduced *Dr* expression in the genital disc using RNAi and visualized a *lacZ* enhancer trap that faithfully reports *bnl* expression (Ahmad and Baker, 2002). In male discs expressing *Dr* RNAi driven by a disc-specific *Gal4*

driver (+/NP6333-Gal4; UAS-*DrRNAi*, UAS-*Dcr-2/bnl-lacZ*), *lacZ* expression was dramatically reduced relative to controls lacking the UAS constructs (Fig. 5E,F). This regulation is cell-autonomous: *Dr* RNAi clones that intersected the normal *bnl* expression domain dramatically reduced *lacZ* expression (Fig. 5G).

Despite their major reduction in *bnl* expression, discs with NP6333-driven RNAi have normal morphologies (Fig. 5F). This unexpected lack of effect on mesodermal cell recruitment could be caused by late RNAi activation by NP6333-Gal4. That is, *Dr* (and therefore *bnl*) expression could have been sufficiently high earlier in larval development, when the recruitment occurs (Ahmad and Baker, 2002). Large clones expressing *Dr* RNAi support this inference: clones that entirely eliminated *bnl* expression on one side of the disc (Fig. 5H) also caused a lack of mesodermal cell recruitment and therefore a malformation of that side (Fig. 5I).

Ahmad and Baker (Ahmad and Baker, 2002) observed that putatively *dsx*-null genital discs [*dsx*^{ts1}/*Df(3R)dsx15*] not only show *bnl* expression in the A9 primordium, but also ectopic expression in A8, which appeared to recruit additional sets of *btl*-expressing

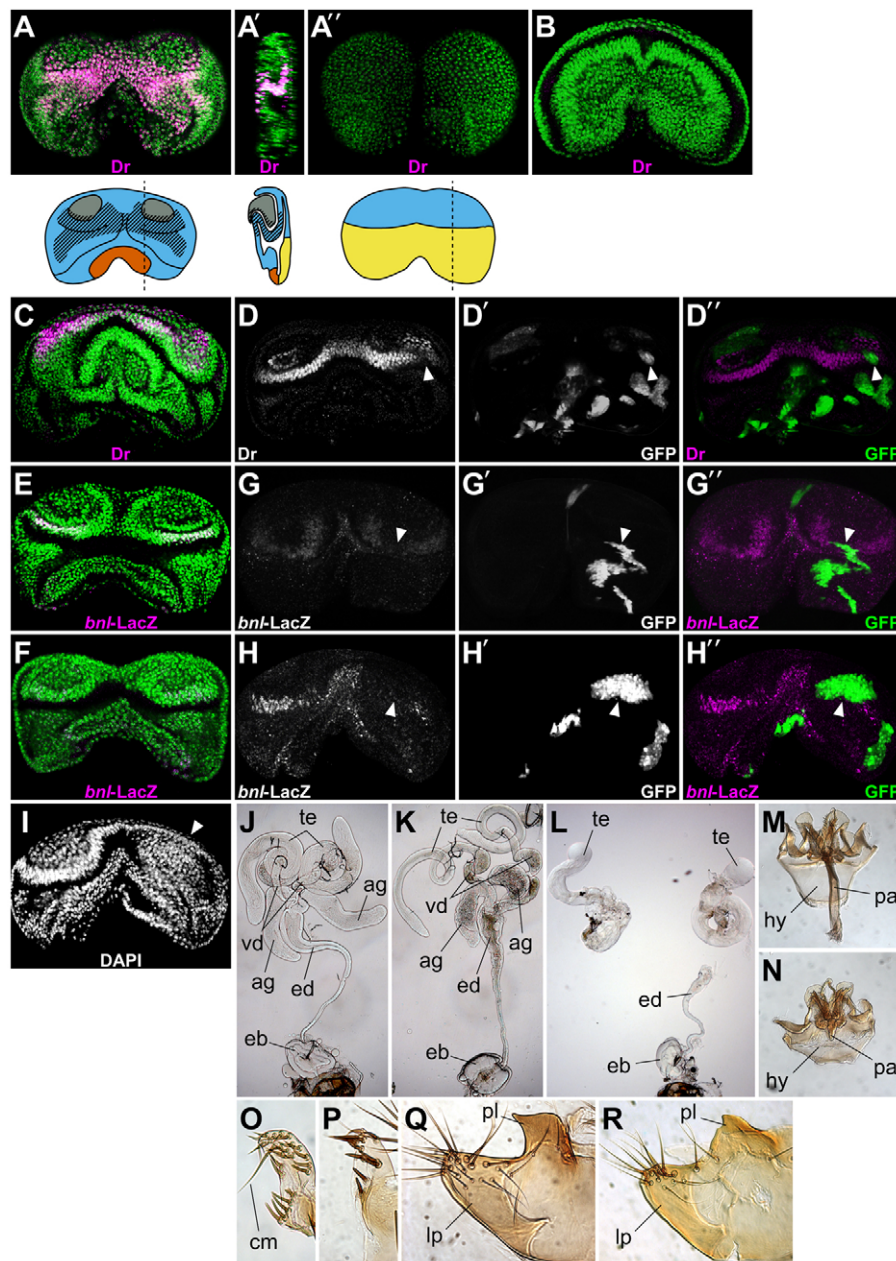


Fig. 5. Sex-specific expression, regulation and function of *Dr*. (A-C) Anti-*Dr* immunofluorescence (magenta). Shown are a confocal slice near the ventral face of the male disc (A), a reconstructed parasagittal section (A') and a confocal slice near the dorsal face (A''). Schematics beneath are as for *Lz* in Fig. 4. (B) Representative confocal slice toward the ventral surface of the female disc. (C) Representative confocal slice toward the ventral surface of a *dsx*-null genital disc. (D-D'') Reduced *Dr* expression in a feminized clone (arrowhead). *Dr* expression (D) and GFP-marked clones (D') are shown individually, then merged in magenta and green, respectively (D''). (E) Expression of *bnl* in control +/NP6333-Gal4; +/*bnl-lacZ* male disc. (F) Reduced expression of *bnl* in +/NP6333-Gal4; *UAS-DrRNAi*; *UAS-Dcr-2/bnl-lacZ* RNAi male disc. (G-G'') Reduced *bnl* expression in a *Dr* RNAi clone. Expression of *bnl-lacZ* (G) and GFP-marked clones (G') are shown individually, then merged in magenta and green, respectively (G''). The arrowhead marks a clone that intersects the normal *bnl* expression domain. (H-H'') Analogous panels to G-G'' showing a larger *Dr* RNAi clone. (I) DAPI staining of the disc in H showing malformation (arrowhead). (J-L) Internal genitalia of +/CyO; *UAS-DrRNAi*, *UAS-Dcr-2/+* control male (J) and +/NP6333-Gal4; *UAS-DrRNAi*, *UAS-Dcr-2/+* RNAi male (K,L). (M-R) Hypandrium and penis apparatus (M,N), clasper (O,P) and posterior lobe and lateral plate (Q,R) of control (M,O,Q) and RNAi (N,P,R) males. Nuclei in A-C,E,F are counterstained with DAPI (green). te, testis; lp, lateral plate; pl, posterior lobe; cm, clasper mechanosensory bristle; other abbreviations as in Fig. 1.

cells. The ectopic *bnl* expression was observed in virtually all *dsx* mutant discs, as were the abutting *btl*-expressing cells; the latter formed deeply invaginating pockets in 20–25% of *dsx* mutant discs (S. Ahmad, personal communication). Because a high percentage of *dsx* mutant animals had been observed to have more than two male accessory glands [62% of *dsx*^l mutants (Hildreth, 1965)], Ahmad and Baker (Ahmad and Baker, 2002) concluded that these extra pockets gave rise to the extra glands. Despite examining ~20 *dsx*-null genital discs, we never observed *Dr* expression in the A8 primordium (Fig. 5C). Likewise, despite examining ~20 *Df(3R)f00683-d07058/Df(3R)dsx15*, *bnl-lacZ* discs, we never observed *lacZ* expression in the A8 primordium. Moreover, in neither case did we ever observe extra mesodermal cell pockets of any depth. We therefore reasoned that, as with *lz*, a difference in *dsx* genotype was causing the discrepancy. We examined 50 *Df(3R)f00683-d07058/Df(3R)dsx15* and 50 *Df(3R)f00683-d07058/Df(3R)dsx15* mutants and found that all had

exactly two male accessory glands. The occasional presence of extra male accessory glands in some *dsx* mutants, like the occasional presence of spermathecae, might therefore be due to residual (and potentially neomorphic) *dsx* activity. This is a plausible explanation as *dsx* coding sequence is present and transcribed in both *dsx*^l and *dsx*²³ (data not shown). All *dsx* exons are present in *dsx*^l. In *dsx*²³, exons 1–3 (including the sequence encoding the Dsx DNA-binding domain) are present, whereas the remaining exons are absent, consistent with a prior report that *dsx*²³ produces a shortened transcript (An and Wensink, 1995).

***Dr* is required for proper development of internal and external male genital structures**

Because *Dr* is required for *bnl* expression in the male disc, and because the *bnl*-recruited mesodermal cells become the accessory glands and vas deferens, we hypothesized that *Dr* would be required for proper development of these organs. In addition, the

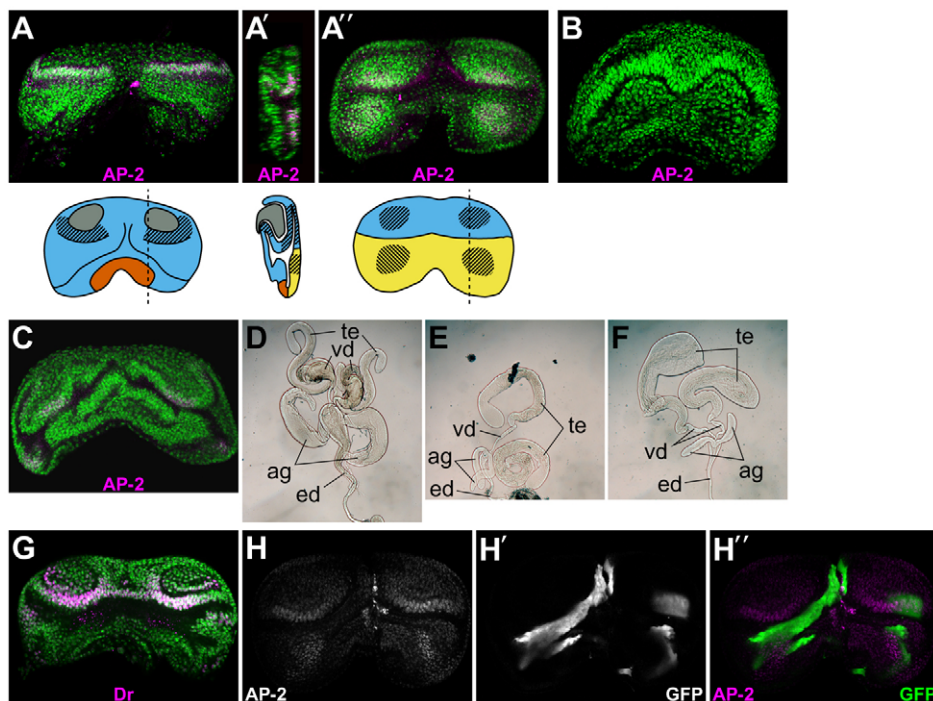


Fig. 6. Sex-specific expression, regulation and function of AP-2.

(A–C) Anti-AP-2 immunofluorescence (magenta). Shown are a confocal slice near the ventral face of the male disc (A), a reconstructed parasagittal section (A') and a confocal slice near the dorsal face (A''). Schematics beneath are as for Lz in Fig. 4. (B) Representative confocal slice toward the ventral surface of the female disc. (C) Representative confocal slice toward the dorsal surface of a *dsx*-null disc. (D–F) Internal genitalia of control male (D), *AP-2²/AP-2¹⁵* mutant male (E) and *NP6333-Gal4/UAS-AP-2RNAi; UAS-Dcr-2/+* RNAi male (F). (G) *Dr* (magenta) expression in *AP-2²/AP-2¹⁵* mutant male disc. (H–H'') AP-2 expression in *Dr* RNAi clones. AP-2 expression (H) and GFP-marked clones (H') are shown individually, then merged in magenta and green, respectively (H''). Nuclei in A–C,G are counterstained with DAPI (green). te, testis; other abbreviations as in Fig. 1.

more lateral and posterior domains of *Dr* expression suggested a role in the development of external genital tissues. We examined males expressing disc-specific *Dr* RNAi (+/*NP6333-Gal4; UAS-DrRNAi, UAS-Dcr-2/+*) and their control brothers lacking *NP6333-Gal4* (Fig. 5J–R). Of 40 *Dr* RNAi flies, 25 (~63%) showed deformed ejaculatory ducts, small accessory glands and malformed vas deferens (Fig. 5K). Consistent with the vas deferens defect, these males also exhibit underdeveloped, uncoiled testes (Stern, 1941a; Stern, 1941b; Kozopas et al., 1998). Six of the 40 RNAi flies (15%) had more severe phenotypes in the internal genitalia, including severely deformed ejaculatory ducts, absent accessory glands and absent vas deferens, which in turn caused the testes to be unattached (Fig. 5L).

Dr RNAi also caused defects in external genital structures. The apodeme and hypandrium of the penis apparatus were abnormal in 23 of 30 RNAi males (~77%). Relative to those of control brothers, the apodeme and hypandrium were both smaller and the hypandrial processes were deformed (Fig. 5M,N). The claspers of RNAi males were also smaller, with fewer bristles on average [19.1±0.6 (mean ± s.e.m.) bristles in RNAi males, 22.8±0.4 in controls; two-sided Wilcoxon rank-sum test, $P=0.0034$]. Some RNAi males had far fewer clasper bristles than any control male (Fig. 5O,P). Moreover, as in *dac* mutants (Keisman and Baker, 2001), *Dr* RNAi claspers lacked the long, mechanosensory bristle (Fig. 5O,P). The genital arch was also affected. The RNAi males showed significantly misshapen posterior lobes (Fig. 5Q,R). The lateral plates were also smaller, with fewer bristles between the tip of the lateral plate and the base of posterior lobe (Fig. 5Q,R).

AP-2 is repressed by DsxF and required for proper male genital morphogenesis

AP-2 is expressed exclusively in the male disc, in three domains (Fig. 6A,B): (1) in the A9 primordium in a medial domain on the ventral surface that encompasses the *bnl*-expressing cells; (2) in the center of each half of the dorsal side of the A9 primordium; and (3) in the center of each half of the A10 primordium. To determine

whether and how the sex-determination hierarchy controls male-specific expression of *AP-2*, we examined *Df(3R)f00683-d07058/Df(3R)f01649-d09625* animals. *AP-2* is expressed in *dsx*-null discs, implying that DsxF normally represses *AP-2* in the female genital disc (Fig. 6C). We examined the effects of loss of *AP-2* function with mutants that survive to pharate adults (*AP-2²/AP-2¹⁵*) (Monge et al., 2001) and with RNAi (Fig. 6D–F). In *AP-2* mutants, relative to wild-type controls, the accessory glands were reduced more than 50%, the vas deferens were narrower at their distal ends and the anterior ejaculatory duct was less bulbous (Fig. 6D,E). Similar phenotypes were observed with *NP6333*-driven *AP-2* RNAi and not in control brothers lacking the driver. Of 30 RNAi males (*NP6333-Gal4/UAS-AP-2RNAi; UAS-Dcr-2/+*), 23 (~77%) showed accessory glands that were similar in size to those of *AP-2²/AP-2¹⁵* males (Fig. 6F). Seven of these 23 showed severely deformed accessory glands and vas deferens, with unattached or underdeveloped testes, similar to the most severe phenotypes seen with *Dr* RNAi. Nineteen of the 30 (~63%) RNAi males also showed deformed or underdeveloped ejaculatory ducts (Fig. 6F).

Dr and *AP-2* are independently regulated by Dsx

Because *Dr* expression and *AP-2* expression overlap on the ventral surface of the A9 primordium of the male disc, and because their loss-of-function phenotypes overlap, we examined whether either regulates the other. In genital discs of male *AP-2* mutants (*AP-2²/AP-2¹⁵*), *Dr* expression was unaffected (Fig. 6G). Likewise, *AP-2* expression was unaffected in *Dr* RNAi clones (Fig. 6H). These results imply that Dsx controls *Dr* and *AP-2* expression in parallel, rather than through a linear pathway.

DISCUSSION

A common theme in the evolution of development is that a limited ‘toolkit’ of regulatory factors is deployed for different purposes during morphogenesis (Carroll et al., 2001). It is therefore not surprising that the key regulators of genital morphogenesis we identified are pleiotropic factors with roles in other developmental

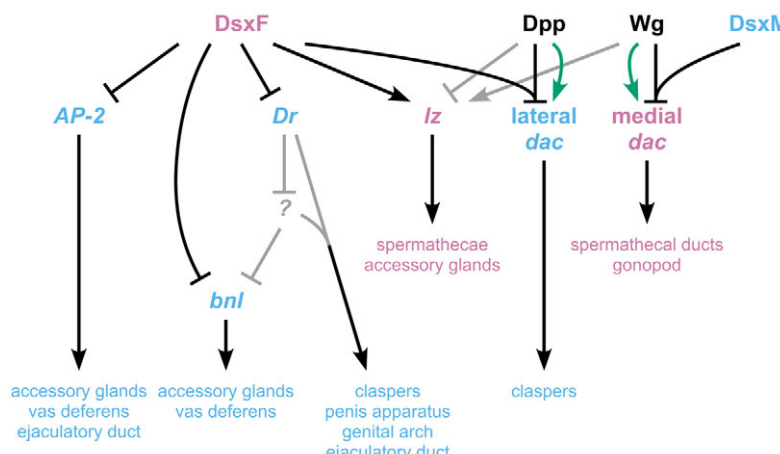


Fig. 7. Control of *Drosophila* sex-specific genital development by *dsx*. Genes or proteins that are active in females or males, and the genital structures that require their functions, are in pink or blue, respectively. The different *dac* expression domains (lateral in males, medial in females) are shown separately in order to indicate their different regulatory inputs, with effects of Dpp or Wg that occur without *Dsx* repression in green. Hypothetical genes (indicated by a question mark) and interactions are in gray.

processes. Fig. 7 presents our current understanding of how *dsx* controls the sex-specific deployment of regulatory factors in the genital disc and, thereby, the development of sex-specific structures. To the two previously established genes downstream of *dsx* in the genital disc (*bnl* and *dac*), we add three new genes: *liz*, *Dr* and *AP-2*.

As with *bnl* and *dac*, it remains to be determined whether these downstream genes are direct *Dsx* targets. Each contains at least one match within an intron to the consensus *Dsx* binding sequence ACAATGT. Future work will determine whether these matches are indeed contained within *Dsx*-regulated genital disc enhancers. Moreover, efforts are underway to define *Dsx* binding locations genome-wide through experiments rather than bioinformatics (B. Baker and D. Luo, personal communication); combined with our expression data, these binding data could speed the discovery of a large number of sex-regulated genital disc enhancers.

An important future direction will be to determine how spatial and temporal cues are integrated with *dsx* to regulate downstream genes. Because *liz* is expressed in the anterior medial region of the female disc, we hypothesize that, like *dac*, it is activated by *Wg* and repressed by *Dpp* (Fig. 7). Such combinatorial regulation could explain the spatially restricted competence of cells in the male disc to activate *liz* in response to *DsxF*. Although *Dr*, *AP-2* and *liz* are expressed at L3, P6 and P20, many other genes are differentially expressed at only one or two of these time points. How these timing differences are regulated is an important unanswered question, especially for genes such as *ac*, which shifts from highly female biased at P6 to highly male biased at P20. Our finding that *Dsx* binding sites are most enriched in genes with sex-biased expression at L3 suggests that indirect regulation through a cascade of interactions might contribute to expression timing differences.

We have already shown that *DsxF* indirectly represses *bnl* by repressing *Dr*. To date, *Dr* has been shown to repress, but not activate, transcription (Ramos and Robert, 2005). Therefore, activation of *bnl* by *Dr* might itself be indirect, via repression of a repressor (Fig. 7). The regulation of *bnl* by *Dr* is sufficient to explain the sex-specific expression of *bnl*. However, upstream of *bnl* are two sequence clusters that match the consensus binding motif of *Dsx* (Ahmad and Baker, 2002). Thus, *bnl* might be repressed both directly and indirectly by *Dsx*, in a coherent feed-forward loop (FFL). FFLs attenuate noisy input signals (Shen-Orr et al., 2002). An FFL emanating from *Dsx* could provide a mechanism of robustly preventing *bnl* activation in female discs, despite potential fluctuations in *DsxF* levels.

Understanding how *Dr* controls the morphogenesis of external structures is also important. The posterior lobe will be of particular interest because it is the most rapidly evolving morphological feature between *D. melanogaster* and its sibling species (Coyle, 1983). Mutations in *Poxn* and *sal* also impair posterior lobe development (Boll and Noll, 2002; Dong et al., 2003). Understanding how these two regulators work with *Dr* to specify and pattern the developing posterior lobe could substantially advance efforts to understand its morphological divergence. Likewise, understanding how *liz* governs spermathecal development could advance evolutionary studies, as this organ also shows rapid evolution (Pitnick et al., 1999).

The extent to which the regulators that we have identified play deeply conserved roles in genital development remains to be determined. Although sex-determination mechanisms evolve rapidly, some features are shared by divergent animal lineages (Marín and Baker, 1998; Zarkower, 2002; Siegal and Baker, 2005; Williams and Carroll, 2009). The observation that FGF signaling is crucial to male differentiation in mammals (Brennan and Capel, 2004), or that mutations in a human *sal* homolog cause anogenital defects (Dong et al., 2003), could reflect ancient roles in genital development or convergent draws from the toolkit.

Whether *AP-2*, *Dr* and *liz* play conserved roles in vertebrate sexual development is similarly uncertain. In mice, an *AP-2* homolog is expressed in the urogenital epithelium (albeit in both sexes) and at least one *AP-2* homolog shows sexually dimorphic expression (albeit in the brain) (Coelho et al., 2005). The mouse *Dr* homolog *Msx1* is expressed in the genital ridge (MacKenzie et al., 1997) and *Msx2* functions in female reproductive tract development (Yin et al., 2006). In chick embryos, *Msx1* and *Msx2* are expressed male specifically in the Müllerian ducts (Ha et al., 2008). The mouse *liz* homolog *Aml1* (*Runx1*) is expressed in the Müllerian ducts and genital tubercle (Simeone et al., 1995). As more data accumulate on the genetic mechanisms controlling genital development in other taxa, the question of how deeply these mechanisms are conserved might be resolved.

Acknowledgements

We thank M. Arbeitman, E. Bach, B. Baker, W. Brook, G. Campbell, A. Christiansen, S. Cohen, C. Desplan, T. Erclik, P. Mitchell, A. Nose, T. Von Ohlen, C. Robinett, A. Shingleton, J. Treisman, the Bloomington *Drosophila* Stock Center, the Developmental Studies Hybridoma Bank and Vienna *Drosophila* RNAi Center for flies and reagents; M. Arbeitman, E. Bach, C. Bertet, K. Birnbaum, J. Blau, R. Bonneau, R. Johnston, A. Madar, J. P. Masly, M. Rosenberg, S. Schnakenberg, I. Tan and M.L.S. lab members for helpful discussions; and three anonymous reviewers for helpful comments. This work

was supported by an Alfred P. Sloan Research Fellowship and an NYU Whitehead Fellowship to M.L.S. M.A.C. was supported by the NYU Dean's Undergraduate Research Fund as a J. S. Sinclair Research Scholar.

Competing interests statement

The authors declare no competing financial interests.

Supplementary material

Supplementary material for this article is available at
<http://dev.biologists.org/lookup/suppl/doi:10.1242/dev.055731/-DC1>

References

- Ahmad, S. M. and Baker, B. S. (2002). Sex-specific deployment of FGF signaling in Drosophila recruits mesodermal cells into the male genital imaginal disc. *Cell* **109**, 651-661.
- An, W. and Wensink, P. C. (1995). Integrating sex- and tissue-specific regulation within a single Drosophila enhancer. *Genes Dev.* **9**, 256-266.
- Anderson, R. C. (1945). A study of the factors affecting fertility of lozenge females of *Drosophila melanogaster*. *Genetics* **30**, 280-296.
- Arbeitman, M. N., Fleming, A. A., Siegal, M. L., Null, B. H. and Baker, B. S. (2004). A genomic analysis of *Drosophila* somatic sexual differentiation and its regulation. *Development* **131**, 2007-2021.
- Arbeitman, M. N., Kopp, A., Siegal, M. L. and Van Doren, M. (2010). Everything you always wanted to know about sex... in flies. *Sex. Dev.* **4**, 315-320.
- Artero, R., Furlong, E. E., Beckett, K., Scott, M. P. and Baylies, M. (2003). Notch and Ras signaling pathway effector genes expressed in fusion competent and founder cells during *Drosophila* myogenesis. *Development* **130**, 6257-6272.
- Bainbridge, S. P. and Bownes, M. (1981). Staging the metamorphosis of *Drosophila melanogaster*. *J. Embryol. Exp. Morphol.* **66**, 57-80.
- Bashaw, G. J. and Baker, B. S. (1997). The regulation of the *Drosophila msl-2* gene reveals a function for Sex-lethal in translational control. *Cell* **89**, 789-798.
- Boll, W. and Noll, M. (2002). The *Drosophila* Pox neuro gene: control of male courtship behavior and fertility as revealed by a complete dissection of all enhancers. *Development* **129**, 5667-5681.
- Bownes, M. (1994). The regulation of the yolk protein genes, a family of sex differentiation genes in *Drosophila melanogaster*. *BioEssays* **16**, 745-752.
- Brennan, J. and Capel, B. (2004). One tissue, two fates: molecular genetic events that underlie testis versus ovary development. *Nat. Rev. Genet.* **5**, 509-521.
- Bryant, P. J. (1978). Pattern formation in imaginal discs. In *The Genetics and Biology of Drosophila*, Vol. 2c (ed. M. Ashburner and T. R. F. Wright), pp. 229-335. New York: Academic Press.
- Burtis, K. C., Coschigano, K. T., Baker, B. S. and Wensink, P. C. (1991). The doublesex proteins of *Drosophila melanogaster* bind directly to a sex-specific yolk protein gene enhancer. *EMBO J.* **10**, 2577-2582.
- Camara, N., Whitworth, C. and Van Doren, M. (2008). The creation of sexual dimorphism in the *Drosophila* soma. *Curr. Top. Dev. Biol.* **83**, 65-107.
- Campbell, G., Weaver, T. and Tomlinson, A. (1993). Axis specification in the developing *Drosophila* appendage: the role of wingless, decapentaplegic, and the homeobox gene aristaless. *Cell* **74**, 1113-1123.
- Canon, J. and Banerjee, U. (2000). Runt and lozenge function in *Drosophila* development. *Semin. Cell Dev. Biol.* **11**, 327-336.
- Carroll, S. B., Grenier, J. K. and Weatherbee, S. D. (2001). *From DNA to Diversity: Molecular Genetics and the Evolution of Animal Design*. Malden, MA: Blackwell Science.
- Casares, F., Sánchez, L., Guerrero, I. and Sánchez-Herrero, E. (1997). The genital disc of *Drosophila melanogaster*. I. Segmental and compartmental organization. *Dev. Genes Evol.* **207**, 216-228.
- Chen, E. H. and Baker, B. S. (1997). Compartmental organization of the *Drosophila* genital imaginal discs. *Development* **124**, 205-218.
- Chen, E. H., Christiansen, A. E. and Baker, B. S. (2005). Allocation and specification of the genital disc precursor cells in *Drosophila*. *Dev. Biol.* **281**, 270-285.
- Christiansen, A. E., Keisman, E. L., Ahmad, S. M. and Baker, B. S. (2002). Sex comes from the cold: the integration of sex and pattern. *Trends Genet.* **18**, 510-516.
- Cline, T. W. and Meyer, B. J. (1996). Vive la difference: males vs females in flies vs worms. *Annu. Rev. Genet.* **30**, 637-702.
- Coelho, D. J., Sims, D. J., Ruegg, P. J., Minn, I., Muensch, A. R. and Mitchell, P. J. (2005). Cell type-specific and sexually dimorphic expression of transcription factor AP-2 in the adult mouse brain. *Neuroscience* **134**, 907-919.
- Cohen, S. M. (1993). Imaginal disc development. In *The Development of Drosophila melanogaster* (ed. M. Bate and A. Martinez-Arias), pp. 747-842. Plainview, NY: Cold Spring Harbor Laboratory Press.
- Couderc, J. L., Godt, D., Zollman, S., Chen, J., Li, M., Tiong, S., Cramton, S. E., Sahut-Barnola, I. and Laski, F. A. (2002). The bric a brac locus consists of two paralogous genes encoding BTB/POZ domain proteins and acts as a homeotic and morphogenetic regulator of imaginal development in *Drosophila*. *Development* **129**, 2419-2433.
- Coyne, J. A. (1983). Genetic basis of differences in genital morphology among three sibling species of *Drosophila*. *Evolution* **37**, 1101-1118.
- Da Lage, J. L., Renard, E., Chartois, F., Lemeunier, F. and Cariou, M. L. (1998). Amyrel, a paralogous gene of the amylase gene family in *Drosophila melanogaster* and the *Sophophora* subgenus. *Proc. Natl. Acad. Sci. USA* **95**, 6848-6853.
- Dietzl, G., Chen, D., Schnorrer, F., Su, K. C., Barinova, Y., Fellner, M., Gasser, B., Kinsey, K., Oppel, S., Scheiblauer, S. et al. (2007). A genome-wide transgenic RNAi library for conditional gene inactivation in *Drosophila*. *Nature* **448**, 151-156.
- Dong, P. D., Todt, S. V., Eberl, D. F. and Boekhoff-Falk, G. (2003). *Drosophila spalt/spalt-related* mutants exhibit Townes-Brocks' syndrome phenotypes. *Proc. Natl. Acad. Sci. USA* **100**, 10293-10298.
- Dorus, S., Busby, S. A., Gerike, U., Shabanowitz, J., Hunt, D. F. and Karr, T. L. (2006). Genomic and functional evolution of the *Drosophila melanogaster* sperm proteome. *Nat. Genet.* **38**, 1440-1445.
- Epper, F. (1983). The evagination of the genital imaginal discs of *Drosophila melanogaster*. I. Morphogenesis of the female genital disc. *Roux Arch. Dev. Biol.* **192**, 275-279.
- Erdman, S. E., Chen, H. J. and Burtis, K. C. (1996). Functional and genetic characterization of the oligomerization and DNA binding properties of the *Drosophila* doublesex proteins. *Genetics* **144**, 1639-1652.
- Estrada, B., Casares, F. and Sanchez-Herrero, E. (2003). Development of the genitalia in *Drosophila melanogaster*. *Differentiation* **71**, 299-310.
- Ferveur, J. F., Stortkuhl, K. F., Stocker, R. F. and Greenspan, R. J. (1995). Genetic feminization of brain structures and changed sexual orientation in male *Drosophila*. *Science* **267**, 902-905.
- Fortier, E. and Belote, J. M. (2000). Temperature-dependent gene silencing by an expressed inverted repeat in *Drosophila*. *Genesis* **26**, 240-244.
- Freeland, D. E. and Kuhn, D. T. (1996). Expression patterns of developmental genes reveal segment and parasegment organization of *D. melanogaster* genital discs. *Mech. Dev.* **56**, 61-72.
- Furlong, E. E. (2004). Integrating transcriptional and signalling networks during muscle development. *Curr. Opin. Genet. Dev.* **14**, 343-350.
- Gentleman, R. C., Carey, V. J., Bates, D. M., Bolstad, B., Dettling, M., Dudoit, S., Ellis, B., Gautier, L., Ge, Y., Gentry, J. et al. (2004). Bioconductor: open software development for computational biology and bioinformatics. *Genome Biol.* **5**, R80.
- Goldman, T. D. and Arbeitman, M. N. (2007). Genomic and functional studies of *Drosophila* sex hierarchy regulated gene expression in adult head and nervous system tissues. *PLoS Genet.* **3**, e216.
- Gorfinkel, N., Sanchez, L. and Guerrero, I. (1999). *Drosophila terminalia* as an appendage-like structure. *Mech. Dev.* **86**, 113-123.
- Ha, Y., Tsukada, A., Saito, N., Zadworny, D. and Shimada, K. (2008). Identification of differentially expressed genes involved in the regression and development of the chicken Mullerian duct. *Int. J. Dev. Biol.* **52**, 1135-1141.
- Hempel, L. U. and Oliver, B. (2007). Sex-specific DoublesexM expression in subsets of *Drosophila* somatic gonad cells. *BMC Dev. Biol.* **7**, 113.
- Hildreth, P. E. (1965). Doublesex, recessive gene that transforms both males and females of *Drosophila* into intersexes. *Genetics* **51**, 659-678.
- Iriaray, R. A., Bolstad, B. M., Collin, F., Cope, L. M., Hobbs, B. and Speed, T. P. (2003). Summaries of Affymetrix GeneChip probe level data. *Nucleic Acids Res.* **31**, e15.
- Ito, K., Awano, W., Suzuki, K., Hiromi, Y. and Yamamoto, D. (1997). The *Drosophila* mushroom body is a quadruple structure of clonal units each of which contains a virtually identical set of neurones and glial cells. *Development* **124**, 761-771.
- Kaufman, L. and Rousseeuw, P. J. (1990). Partitioning around medoids (Program PAM). In *Finding Groups in Data: An Introduction to Cluster Analysis*, pp. 68-125. New York, NY: Wiley.
- Keisman, E. L. and Baker, B. S. (2001). The *Drosophila* sex determination hierarchy modulates wingless and decapentaplegic signaling to deploy dachshund sex-specifically in the genital imaginal disc. *Development* **128**, 1643-1656.
- Keisman, E. L., Christiansen, A. E. and Baker, B. S. (2001). The sex determination gene doublesex regulates the A/P organizer to direct sex-specific patterns of growth in the *Drosophila* genital imaginal disc. *Dev. Cell* **1**, 215-225.
- Kiger, J. A., Jr, Natzke, J. E., Kimbrell, D. A., Paddy, M. R., Kleinhesselink, K. and Green, M. M. (2007). Tissue remodeling during maturation of the *Drosophila* wing. *Dev. Biol.* **301**, 178-191.
- Kopp, A., Duncan, I., Godt, D. and Carroll, S. B. (2000). Genetic control and evolution of sexually dimorphic characters in *Drosophila*. *Nature* **408**, 553-559.
- Kosman, D., Mizutani, C. M., Lemons, D., Cox, W. G., McGinnis, W. and Bier, E. (2004). Multiplex detection of RNA expression in *Drosophila* embryos. *Science* **305**, 846.
- Kozopas, K. M., Samos, C. H. and Nusse, R. (1998). DWnt-2, a *Drosophila* Wnt gene required for the development of the male reproductive tract, specifies a sexually dimorphic cell fate. *Genes Dev.* **12**, 1155-1165.

- Lebo, M. S., Sanders, L. E., Sun, F. and Arbeitman, M. N.** (2009). Somatic, germline and sex hierarchy regulated gene expression during *Drosophila* metamorphosis. *BMC Genomics* **10**, 80.
- MacKenzie, A., Purdie, L., Davidson, D., Collinson, M. and Hill, R. E.** (1997). Two enhancer domains control early aspects of the complex expression pattern of *Msx1*. *Mech. Dev.* **62**, 29-40.
- Manolakou, P., Lavranos, G. and Angelopoulou, R.** (2006). Molecular patterns of sex determination in the animal kingdom: a comparative study of the biology of reproduction. *Reprod. Biol. Endocrinol.* **4**, 59.
- Marín, I. and Baker, B. S.** (1998). The evolutionary dynamics of sex determination. *Science* **281**, 1990-1994.
- Milán, M., Weihe, U., Tiong, S., Bender, W. and Cohen, S. M.** (2001). *msh* specifies dorsal cell fate in the *Drosophila* wing. *Development* **128**, 3263-3268.
- Monge, I., Krishnamurthy, R., Sims, D., Hirth, F., Spengler, M., Kammermeier, L., Reichert, H. and Mitchell, P. J.** (2001). *Drosophila* transcription factor AP-2 in proboscis, leg and brain central complex development. *Development* **128**, 1239-1252.
- Nöthiger, R., Dübendorfer, A. and Epper, F.** (1977). Gynandromorphs reveal two separate primordia for male and female genitalia. *Roux's Arch. Dev. Biol.* **181**, 367-373.
- Parks, A. L., Cook, K. R., Belvin, M., Dompe, N. A., Fawcett, R., Huppert, K., Tan, L. R., Winter, C. G., Bogart, K. P., Deal, J. E. et al.** (2004). Systematic generation of high-resolution deletion coverage of the *Drosophila melanogaster* genome. *Nat. Genet.* **36**, 288-292.
- Pignoni, F. and Zipursky, S. L.** (1997). Induction of *Drosophila* eye development by decapentaplegic. *Development* **124**, 271-278.
- Pitnick, S., Markow, T. and Spicer, G. S.** (1999). Evolution of multiple kinds of female sperm-storage organs in *Drosophila*. *Evolution* **53**, 1804-1822.
- Ramos, C. and Robert, B.** (2005). *msh/Msx* gene family in neural development. *Trends Genet.* **21**, 624-632.
- Robinett, C. C., Vaughan, A. G., Knapp, J. M. and Baker, B. S.** (2010). Sex and the single cell. II. There is a time and place for sex. *PLoS Biol.* **8**, e1000365.
- Schüpbach, T., Wieschaus, E. and Nöthiger, R.** (1978). The embryonic organization of the genital disc studied in genetic mosaics of *Drosophila melanogaster*. *Roux's Arch. Dev. Biol.* **185**, 249-270.
- Shen-Orr, S. S., Milo, R., Mangan, S. and Alon, U.** (2002). Network motifs in the transcriptional regulation network of *Escherichia coli*. *Nat. Genet.* **31**, 64-68.
- Shirangi, T. R., Dufour, H. D., Williams, T. M. and Carroll, S. B.** (2009). Rapid evolution of sex pheromone-producing enzyme expression in *Drosophila*. *PLoS Biol.* **7**, e1000168.
- Siegal, M. L. and Baker, B. S.** (2005). Functional conservation and divergence of intersex, a gene required for female differentiation in *Drosophila melanogaster*. *Dev. Genes Evol.* **215**, 1-12.
- Simeone, A., Daga, A. and Calabi, F.** (1995). Expression of runt in the mouse embryo. *Dev. Dyn.* **203**, 61-70.
- Skeath, J. B. and Carroll, S. B.** (1991). Regulation of achaete-scute gene expression and sensory organ pattern formation in the *Drosophila* wing. *Genes Dev.* **5**, 984-995.
- Sosinsky, A., Bonin, C. P., Mann, R. S. and Honig, B.** (2003). Target explorer: An automated tool for the identification of new target genes for a specified set of transcription factors. *Nucleic Acids Res.* **31**, 3589-3592.
- Spéder, P., Ádám, G. and Noselli, S.** (2006). Type ID unconventional myosin controls left-right asymmetry in *Drosophila*. *Nature* **440**, 803-807.
- Stern, C.** (1941a). The growth of the testes in *Drosophila*. I. The relation between vas deferens and testis within various species. *J. Exp. Zool.* **87**, 113-158.
- Stern, C.** (1941b). The growth of the testes in *Drosophila*. II. The nature of interspecific differences. *J. Exp. Zool.* **87**, 159-180.
- Stieper, B. C., Kupershtok, M., Driscoll, M. V. and Shingleton, A. W.** (2008). Imaginal discs regulate developmental timing in *Drosophila melanogaster*. *Dev. Biol.* **321**, 18-26.
- Sullivan, W., Ashburner, M. and Hawley, R. S.** (2000). *Drosophila Protocols*. Cold Spring Harbor, NY: Cold Spring Harbor Laboratory Press.
- Suzanne, M., Petzoldt, A. G., Spéder, P., Coutelis, J. B., Steller, H. and Noselli, S.** (2010). Coupling of apoptosis and L/R patterning controls stepwise organ looping. *Curr. Biol.* **20**, 1773-1778.
- Takemori, N. and Yamamoto, M. T.** (2009). Proteome mapping of the *Drosophila melanogaster* male reproductive system. *Proteomics* **9**, 2484-2493.
- Tusher, V. G., Tibshirani, R. and Chu, G.** (2001). Significance analysis of microarrays applied to the ionizing radiation response. *Proc. Natl. Acad. Sci. USA* **98**, 5116-5121.
- Tweedie, S., Ashburner, M., Falls, K., Leyland, P., McQuilton, P., Marygold, S., Millburn, G., Osumi-Sutherland, D., Schroeder, A., Seal, R. et al.** (2009). FlyBase: enhancing *Drosophila* gene ontology annotations. *Nucleic Acids Res.* **37**, D555-D559.
- van der Laan, M. J., Pollard, K. S. and Bryan, J.** (2003). A new partitioning around medoids algorithm. *J. Stat. Comput. Simul.* **73**, 575-584.
- von Ohlen, T. and Doe, C. Q.** (2000). Convergence of dorsal, dpp, and egfr signaling pathways subdivides the *drosophila* neuroectoderm into three dorsal-ventral columns. *Dev. Biol.* **224**, 362-372.
- Williams, T. M. and Carroll, S. B.** (2009). Genetic and molecular insights into the development and evolution of sexual dimorphism. *Nat. Rev. Genet.* **10**, 797-804.
- Williams, T. M., Selegue, J. E., Werner, T., Gompel, N., Kopp, A. and Carroll, S. B.** (2008). The regulation and evolution of a genetic switch controlling sexually dimorphic traits in *Drosophila*. *Cell* **134**, 610-623.
- Xu, T. and Rubin, G. M.** (1993). Analysis of genetic mosaics in developing and adult *Drosophila* tissues. *Development* **117**, 1223-1237.
- Xue, L. and Noll, M.** (2002). Dual role of the Pax gene paired in accessory gland development of *Drosophila*. *Development* **129**, 339-346.
- Yao, J. G., Weasner, B. M., Wang, L. H., Jang, C. C., Weasner, B., Tang, C. Y., Salzer, C. L., Chen, C. H., Hay, B., Sun, Y. H. et al.** (2008). Differential requirements for the Pax6(5a) genes eyegone and twin of eyegone during eye development in *Drosophila*. *Dev. Biol.* **315**, 535-551.
- Yin, Y., Lin, C. and Ma, L.** (2006). MSX2 promotes vaginal epithelial differentiation and Wolffian duct regression and dampens the vaginal response to diethylstilbestrol. *Mol. Endocrinol.* **20**, 1535-1546.
- Zarkower, D.** (2002). Invertebrates may not be so different after all. *Novartis Found. Symp.* **244**, 115-135.

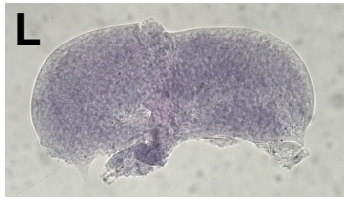
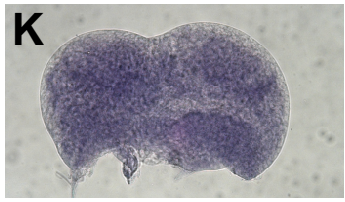
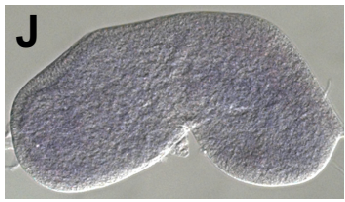
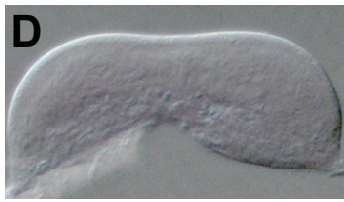
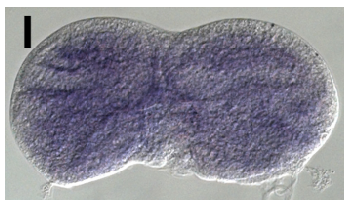
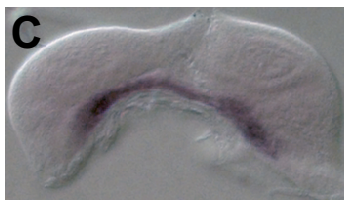
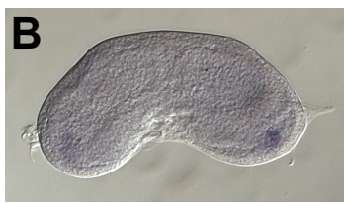
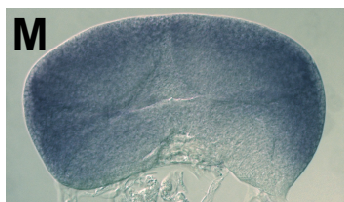
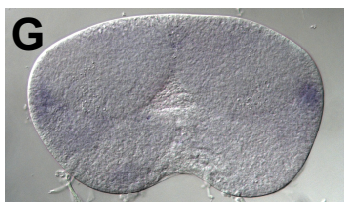
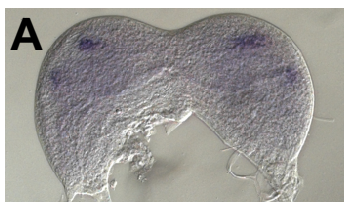


Table S1. cDNA clones and PCR primers used for in situ hybridization probes

Gene	Clone ID*/primers [†]
<i>al</i>	RE68460
<i>ap</i>	SD05617
<i>AP-2</i>	RE17884
<i>CG3355</i>	RE64759
<i>CG4267</i>	RH13166
<i>dpr17</i>	RE56367
<i>Dr</i>	LD04235
<i>Phk-3</i>	RE09339
<i>caup</i>	CCAGAACTTCTATCCACCCCATC CATGACTGTGTCCGTGTCATATC CTTATCATGGCCGGAGCTCTATT CTTAATAACTAGCACCGCCTGTCG
<i>CG1499</i>	AATTAACCCTCACTAAAGGAGAACCTACTACTACGGAGGACG TAATACGACTCACTATAGGTGCGCATCTATTGCTGTGG
<i>CG13053</i>	TTACTCAAACGGCAAACGGCATCG GCAAGTAAACACGTTGAGAGGTCA
<i>CG42749</i>	CATCGACAACACTGGTGCAGAGATCAA CGGGGACACTCCGATTATAGTT
<i>s/p2</i>	ACTGAGGCGCTAGACGCTTGAAA ACCAACTCTGAACACTCGCTGGT
<i>toe</i>	TCCAGTCCAGTTGCAGTTCCAGA TAATGGAGGCTGATGCTGTGGGTGA

*cDNA clones with the specified IDs were obtained from the *Drosophila* Genomics Resource Center (DGRC).

[†]Primer sequences are given 5' to 3'. Each PCR product was cloned into one of the following vectors containing promoter sequences for riboprobe production: pGEM-T Easy (*caup* and *toe*), EcoRV-digested pBluescript II KS+ (*CG1499*, *CG42342*, *CG42749* and *s/p2*) or EcoRV-digested pSLfa1180fa (*CG13053*).

Table S2. Genes sex-differentially expressed at L3

Probe set*	Gene [†]	q-value [‡]	Sex bias	Fold difference
1623776_s_at	<i>dsx</i>	0.0214	F	44.64
1636456_at	<i>CG13053</i>	0.0214	M	46.70
1633299_at	<i>lz</i>	0.0229	F	26.43
1641137_at	<i>Dr</i>	0.0229	M	57.80
1636392_at	<i>CG15785</i>	0.0229	M	6.03
1638037_a_at	<i>dpr17</i>	0.0247	F	10.75
1624802_at	<i>CG31686</i>	0.0247	F	6.64
1637225_at	<i>bni</i>	0.0247	M	9.06
1627053_at	<i>slp2</i>	0.0247	M	5.61
1633383_at	<i>toe</i>	0.0259	F	5.89
1632977_at	<i>Poxn</i>	0.0247	M	10.06
1627135_at	<i>bni</i>	0.0247	M	8.37
1632742_at	<i>eyg</i>	0.0259	F	6.50
1637635_at	<i>CG4766</i>	0.0259	M	7.08
1626934_a_at	<i>wb</i>	0.0259	M	2.44
1633305_at	<i>Obp99a</i>	0.0259	M	5.22
1638132_at	<i>CG10184</i>	0.0292	F	5.68
1626109_a_at	<i>Drip</i>	0.0292	F	4.23
1625940_s_at	<i>sim</i>	0.0292	M	4.61
1637438_at	<i>Wnt2</i>	0.0292	M	5.16
1632317_at	<i>CG3036</i>	0.0292	M	2.02
1623466_at	<i>bab1</i>	0.0327	F	2.90
1636393_at	<i>CG15005</i>	0.0292	M	4.55
1640670_at	<i>btl</i>	0.0292	M	3.34
1639333_at	<i>al</i>	0.0327	F	2.93
1625207_at	<i>CG32636</i>	0.0327	F	2.81
1623910_at	<i>alphaTub85E</i>	0.0327	F	3.63
1631471_at	<i>CG14889</i>	0.0315	M	2.63
1626235_at	<i>m</i>	0.0327	M	4.55
1630120_s_at	—	0.0338	F	2.00
1625621_s_at	<i>f</i>	0.0327	M	2.71
1639483_s_at	<i>Nep1</i>	0.0327	M	3.54
1639535_at	<i>pgant2</i>	0.0338	M	4.73
1624175_at	<i>caup</i>	0.0343	M	3.31
1626388_at	<i>Ctr1B</i>	0.0343	M	3.25
1623006_at	<i>SerT</i>	0.0399	F	3.48
1637813_at	<i>abd-A</i>	0.0399	F	3.22
1626903_at	<i>CG3355</i>	0.0349	M	6.05
1636558_a_at	<i>abd-A</i>	0.0404	F	2.40
1631783_at	<i>CG4267</i>	0.0404	F	9.04
1625341_at	<i>FucTC</i>	0.0399	M	2.73
1640697_at	—	0.0399	M	2.57
1636668_at	<i>CG9972</i>	0.0399	M	3.05
1639776_s_at	<i>CG1499</i>	0.0399	M	3.14
1635840_s_at	<i>msl-2</i>	0.0399	M	2.09
1632591_at	<i>Phk-3</i>	0.0399	M	3.98
1639433_at	<i>dpn</i>	0.0404	M	2.62
1639741_at	<i>HLHm5</i>	0.0414	M	4.74
1624412_at	<i>ap</i>	0.0417	M	2.64
1633377_at	<i>CG40303</i>	0.0426	M	2.92
1625935_at	<i>Trim9</i>	0.0471	M	2.54
1628729_at	<i>vvl</i>	0.0473	M	1.62
1625535_at	<i>H15</i>	0.0496	M	2.05
1631372_a_at	<i>AP-2</i>	0.0514	M	3.63
1639732_s_at	<i>salr</i>	0.0514	M	1.94

*Affymetrix probe set ID.

†Annotated gene corresponding to probe set [if blank (—), the probe set maps to an unannotated region of the genome].

‡The lowest FDR threshold at which the probe set is called significant by SAM.

Table S3. Genes sex-differentially expressed at P6

Probe set*	Gene†	q-value‡	Sex bias	Fold difference
1631783_at	<i>CG4267</i>	0.0166	F	43.17
1631126_at	<i>gcm</i>	0.0166	M	44.90
1623776_s_at	<i>dsx</i>	0.0172	F	25.38
1624802_at	<i>CG31686</i>	0.0172	F	11.46
1640868_at	<i>ato</i>	0.0172	F	8.20
1638324_s_at	<i>CG6921</i>	0.0172	M	7.77
1634063_a_at	<i>stumps</i>	0.0172	M	4.37
1633952_at	<i>CG7080</i>	0.0172	M	2.29
1624932_at	<i>Obp49a</i>	0.0172	M	15.63
1632742_at	<i>eyg</i>	0.0189	F	11.04
1632977_at	<i>Poxn</i>	0.0189	M	9.24
1624989_s_at	<i>Ef1alpha100E</i>	0.0189	F	3.72
1630927_x_at	<i>Pxd</i>	0.0189	F	11.80
1636456_at	<i>CG13053</i>	0.0189	M	10.14
1626799_a_at	<i>CG16758</i>	0.0189	F	1.93
1631372_a_at	<i>AP-2</i>	0.0189	M	7.21
1637311_at	<i>pburs</i>	0.0189	M	14.89
1633341_s_at	<i>dac</i>	0.0189	M	3.28
1624543_s_at	<i>springer transposon</i>	0.0189	M	3.59
1637438_at	<i>Wnt2</i>	0.0189	M	6.65
1637635_at	<i>CG4766</i>	0.0189	M	3.20
1636251_at	<i>Tsp</i>	0.0199	F	2.73
1627194_at	<i>I(1)sc</i>	0.0199	F	8.35
1633387_at	<i>bves</i>	0.0199	F	4.06
1633377_at	<i>CG40303</i>	0.0199	M	5.76
1638888_at	<i>unpg</i>	0.0199	F	6.97
1625510_at	<i>Osi1</i>	0.0199	M	4.29
1623410_at	<i>Pxd</i>	0.0199	F	15.34
1627135_at	<i>bnl</i>	0.0199	M	6.08
1628089_at	<i>ham</i>	0.0199	M	20.72
1632317_at	<i>CG3036</i>	0.0199	M	1.44
1638853_at	<i>CG32971</i>	0.0199	M	3.85
1623206_a_at	<i>eya</i>	0.0199	M	4.67
1636646_at	<i>sna</i>	0.0199	M	5.98
1631222_at	<i>pdm3</i>	0.0199	M	2.33
1637813_at	<i>abd-A</i>	0.0207	F	3.69
1641490_s_at	<i>Tsp</i>	0.0207	F	3.17
1641137_at	<i>Dr</i>	0.0201	M	94.92
1627979_at	<i>Wnt6</i>	0.0207	F	2.90
1634873_at	<i>stumps</i>	0.0201	M	6.85
1623092_at	<i>Pcp</i>	0.0201	M	14.71
1637225_at	<i>bnl</i>	0.0207	M	4.20
1637513_at	<i>CG11275</i>	0.0207	M	2.47
1634054_at	<i>ninaC</i>	0.0207	F	3.82
1638481_at	<i>CG2736</i>	0.0207	M	3.06
1627478_at	<i>CG33232</i>	0.0207	F	1.93
1625341_at	<i>FucTC</i>	0.0207	M	4.50
1628677_at	<i>Pkcdelta</i>	0.0207	F	2.17
1624819_s_at	<i>gypsy transposon</i>	0.0207	F	2.59
1640097_at	<i>Pxn</i>	0.0207	M	1.84
1629048_s_at	<i>CG9674</i>	0.0207	M	1.99
1627681_at	<i>Cpr35B</i>	0.0207	M	3.51
1634526_a_at	<i>qua</i>	0.0207	M	6.57
1640799_at	<i>dsx</i>	0.0207	M	1.80
1631408_at	<i>SoxN</i>	0.0207	M	3.95
1627881_at	<i>salm</i>	0.0207	M	3.26
1639333_at	<i>al</i>	0.0216	F	4.30
1624060_at	<i>bab2</i>	0.0216	F	2.50
1636905_at	<i>lea</i>	0.0216	M	1.72
1633530_at	<i>HGTX</i>	0.0216	M	2.96
1633879_a_at	<i>prd</i>	0.0216	M	3.39
1625913_at	<i>CG9970</i>	0.0216	M	2.13
1636387_at	<i>CG10300</i>	0.0223	F	2.04
1625950_a_at	<i>CG7777</i>	0.0223	F	4.48
1628125_at	<i>Doc2</i>	0.0218	M	2.19
1626388_at	<i>Ctr1B</i>	0.0218	M	5.62
1632019_s_at	<i>CG9008</i>	0.0225	F	2.20
1627445_s_at	<i>en</i>	0.0218	M	1.48
1629733_at	<i>Lim1</i>	0.0225	F	1.49
1623770_at	<i>CG1673</i>	0.0223	M	2.40
1633383_at	<i>toe</i>	0.0225	F	13.85
1632082_at	<i>Ndg</i>	0.0225	F	3.18

1632448_s_at	<i>kel</i>	0.0225	F	3.68
1639734_at	<i>CG4017</i>	0.0225	M	3.04
1623466_at	<i>bab1</i>	0.0225	F	2.37
1624412_at	<i>ap</i>	0.0225	M	4.68
1629446_at	<i>CG1136</i>	0.0228	F	3.57
1629227_at	<i>baz</i>	0.0225	M	2.03
1626934_a_at	<i>wb</i>	0.0225	M	2.80
1636742_at	<i>nord</i>	0.0225	M	3.38
1641236_s_at	<i>CG5758</i>	0.0228	F	3.98
1632372_at	<i>CG31076</i>	0.0228	F	1.79
1627971_s_at	<i>sano</i>	0.0225	M	2.06
1641219_at	<i>CG11136</i>	0.0225	M	1.91
1623395_at	—	0.0225	M	2.60
1626665_at	<i>CG7408</i>	0.0229	F	1.86
1627515_at	<i>CG10641</i>	0.0229	F	1.32
1633591_at	<i>gcm2</i>	0.0228	M	2.74
1640139_at	<i>B-H2</i>	0.0229	F	2.86
1626773_s_at	<i>CG18431</i>	0.0228	M	1.77
1640697_at	—	0.0228	M	2.88
1632868_a_at	<i>wg</i>	0.0235	F	1.78
1640912_s_at	<i>scarface</i>	0.0235	F	2.61
1638592_at	<i>CG6560</i>	0.0228	M	3.08
1631027_at	<i>ara</i>	0.0228	M	4.45
1634250_at	<i>Act57B</i>	0.0235	F	1.93
1639868_at	<i>CG1702</i>	0.0229	M	1.54
1635840_s_at	<i>msl-2</i>	0.0229	M	2.10
1634778_at	<i>CG3092</i>	0.0229	M	1.75
1636688_at	<i>Cyp4s3</i>	0.0229	M	2.46
1631867_at	<i>ldgf5</i>	0.0245	F	1.66
1625321_a_at	<i>CG7549</i>	0.0245	F	2.32
1634211_at	<i>arr</i>	0.0235	M	1.45
1633299_at	<i>lz</i>	0.0246	F	34.69
1623197_a_at	<i>zormin</i>	0.0246	F	2.27
1637755_at	<i>CG10987</i>	0.0246	F	4.53
1635562_at	—	0.0246	F	1.37
1628450_at	<i>Nplp1</i>	0.0245	M	2.97
1625844_s_at	<i>apt</i>	0.0245	M	1.54
1639913_at	<i>Con</i>	0.0246	M	2.35
1626058_at	<i>lbl</i>	0.0265	F	1.46
1631323_a_at	<i>CG2663</i>	0.0246	M	2.14
1638596_at	<i>ac</i>	0.0265	F	1.60
1626831_at	<i>CG6579</i>	0.0265	F	3.43
1625454_at	<i>Gbeta5</i>	0.0250	M	2.13
1632226_at	<i>Fie</i>	0.0273	F	3.90
1639353_at	<i>CG17032</i>	0.0274	F	1.58
1624982_s_at	<i>CG5080</i>	0.0274	F	2.51
1626150_at	<i>tsh</i>	0.0274	F	2.34
1636089_at	<i>comm</i>	0.0265	M	1.48
1623910_at	<i>alphaTub85E</i>	0.0275	F	3.00
1637790_a_at	<i>CG12250</i>	0.0273	M	1.91
1631665_at	<i>Acp76A</i>	0.0275	F	2.38
1625940_s_at	<i>sim</i>	0.0274	M	1.56
1628747_at	—	0.0279	F	1.85
1638821_a_at	<i>yuri</i>	0.0275	M	1.80
1632781_s_at	<i>Abd-B</i>	0.0275	M	1.48
1638961_at	<i>CG14264</i>	0.0279	F	1.27
1635139_at	<i>CG13340</i>	0.0275	M	8.21
1625727_at	<i>CG32006</i>	0.0275	M	1.85
1637869_at	<i>rdo</i>	0.0275	M	1.75
1637049_at	<i>bi</i>	0.0275	M	1.62
1624624_at	<i>mud</i>	0.0275	M	2.51
1626570_s_at	<i>SNF4Agamma</i>	0.0275	M	1.35
1628584_at	<i>Cyp305a1</i>	0.0275	M	2.47
1637638_s_at	<i>CG10702</i>	0.0288	F	1.65
1630570_at	<i>CG13003</i>	0.0279	M	2.02
1629365_at	<i>CG30324</i>	0.0279	M	3.44
1627507_at	<i>CG5704</i>	0.0279	M	1.64
1636558_a_at	<i>abd-A</i>	0.0290	F	4.29
1633748_at	<i>CG2014</i>	0.0279	M	2.11
1636203_at	<i>B-H1</i>	0.0290	F	3.21
1624175_at	<i>caup</i>	0.0279	M	3.72
1631115_at	<i>Obp8a</i>	0.0290	F	1.18
1633032_s_at	<i>CG8177</i>	0.0279	M	1.72
1629670_at	<i>CG17376</i>	0.0279	M	13.95
1639723_at	<i>CG7443</i>	0.0279	M	2.60

1629922_at	<i>CG11409</i>	0.0290	F	1.65
1640867_s_at	<i>htl</i>	0.0290	F	1.68
1637830_s_at	<i>CG31145</i>	0.0290	F	2.26
1632431_s_at	<i>Ance</i>	0.0279	M	2.31
1627432_at	<i>CG6041</i>	0.0279	M	1.98
1640261_at	<i>CG9522</i>	0.0279	M	3.16
1631394_at	<i>CG31324</i>	0.0288	M	2.62
1626451_at	<i>CG13847</i>	0.0301	F	1.95
1631597_at	<i>foxo</i>	0.0289	M	1.57
1629066_at	<i>GRHRII</i>	0.0301	F	3.59
1635127_at	<i>CG34398</i>	0.0301	F	1.57
1637246_a_at	<i>CG32627</i>	0.0290	M	2.47
1639042_at	<i>CG6414</i>	0.0290	M	4.13
1624297_at	<i>drl</i>	0.0290	M	2.72
1639425_at	<i>CG18662</i>	0.0290	M	12.41
1628774_a_at	<i>boi</i>	0.0290	M	1.70
1640235_at	<i>W</i>	0.0290	M	1.75
1637803_s_at	-	0.0315	F	2.07
1634552_at	<i>TepIV</i>	0.0294	M	1.47
1623959_at	<i>CG1532</i>	0.0318	F	1.72
1639636_at	<i>Cht7</i>	0.0295	M	1.84
1627499_at	<i>CG2016</i>	0.0320	F	1.82
1632648_at	<i>CG14681</i>	0.0320	F	1.60
1637021_at	<i>stumps</i>	0.0298	M	1.38
1636969_at	<i>Poxm</i>	0.0301	M	2.10
1624229_at	<i>CG15705</i>	0.0301	M	1.78
1640342_at	<i>CG6234</i>	0.0301	M	1.55
1640513_a_at	<i>CG32150</i>	0.0301	M	1.56
1626470_at	<i>CG10440</i>	0.0301	M	1.81
1632265_at	-	0.0327	F	1.26
1640181_at	<i>CG13044</i>	0.0327	F	2.75
1636364_a_at	<i>CG17376</i>	0.0303	M	22.25
1637078_a_at	<i>Poxm</i>	0.0303	M	1.78
1624521_a_at	<i>CG17896</i>	0.0303	M	1.47
1628604_at	<i>D</i>	0.0303	M	2.53
1636759_at	<i>CG8303</i>	0.0303	M	3.87
1634833_at	<i>PQBP-1</i>	0.0306	M	1.97
1625145_a_at	<i>Anxb11</i>	0.0353	F	1.26
1624699_s_at	<i>Bx</i>	0.0315	M	2.66
1632039_at	<i>CG4546</i>	0.0318	M	2.17
1632993_at	<i>CG6372</i>	0.0320	M	11.97
1639743_s_at	<i>Syn2</i>	0.0362	F	1.84
1638186_a_at	<i>Fem-1</i>	0.0320	M	1.26
1623006_at	<i>SerT</i>	0.0368	F	2.94
1639165_at	<i>Mst84Dd</i>	0.0320	M	7.52
1623707_a_at	<i>CG32192</i>	0.0320	M	4.08
1638441_a_at	<i>CG18519</i>	0.0320	M	1.73
1632688_s_at	<i>CG11594</i>	0.0369	F	1.75
1638284_at	<i>CG3199</i>	0.0327	M	1.62
1627071_at	<i>dpr</i>	0.0375	F	1.68
1629120_at	<i>alpha-Man-I</i>	0.0330	M	1.88
1626723_at	<i>Takr86C</i>	0.0375	F	3.61
1627734_at	<i>nau</i>	0.0380	F	2.49
1633452_a_at	<i>Rya-r44F</i>	0.0381	F	1.62
1634126_at	<i>CG31788</i>	0.0339	M	7.99
1633623_s_at	<i>sano</i>	0.0339	M	1.92
1623909_s_at	<i>inv</i>	0.0339	M	1.60
1626383_at	<i>CG4096</i>	0.0353	M	1.70
1630608_at	<i>CG14608</i>	0.0396	F	1.66
1634261_at	<i>Cyp312a1</i>	0.0356	M	1.47
1633480_at	<i>CG5392</i>	0.0356	M	1.52
1639433_at	<i>dpn</i>	0.0356	M	2.06
1639483_s_at	<i>Nep1</i>	0.0356	M	2.75
1627752_s_at	<i>SK</i>	0.0412	F	2.16
1639732_s_at	<i>salr</i>	0.0356	M	1.90
1636536_at	<i>Pglym87</i>	0.0356	M	1.34
1623978_at	<i>CG10862</i>	0.0356	M	3.00
1624942_at	<i>bab1</i>	0.0425	F	1.47
1639797_at	<i>CG34109</i>	0.0425	F	1.23
1636440_at	<i>Sip1</i>	0.0425	F	1.28
1631497_at	<i>Tsp42Eo</i>	0.0425	F	1.73
1630097_s_at	<i>CG17834</i>	0.0368	M	2.31
1623950_s_at	<i>Ama</i>	0.0425	F	1.37
1625075_at	<i>Nep2</i>	0.0425	F	1.40
1631077_at	<i>CG16957</i>	0.0369	M	1.39

1627808_at	<i>CG13011</i>	0.0425	F	2.43
1626241_at	<i>Cyt-c-d</i>	0.0369	M	2.30
1638907_at	<i>msi</i>	0.0369	M	1.48
1640327_at	<i>CG6023</i>	0.0369	M	2.20
1625220_at	—	0.0425	F	1.18
1624813_s_at	<i>CG34008</i>	0.0370	M	1.26
1638051_at	<i>CG17323</i>	0.0375	M	1.20
1628878_at	<i>al</i>	0.0432	F	3.59
1639106_at	<i>Grip</i>	0.0432	F	1.36
1631346_a_at	<i>CG30412</i>	0.0376	M	1.52
1630337_at	<i>CG15927</i>	0.0376	M	1.93
1634644_at	<i>CG42523</i>	0.0380	M	11.06
1625198_at	<i>ss</i>	0.0438	F	1.71
1626892_at	<i>del</i>	0.0381	M	1.43
1631238_at	<i>Hsp60B</i>	0.0381	M	2.86
1641476_a_at	<i>Timp</i>	0.0447	F	1.57
1629612_at	<i>CG31158</i>	0.0447	F	1.20
1639541_at	—	0.0448	F	1.39
1633893_at	<i>CG31217</i>	0.0450	F	1.42
1641422_at	<i>htt</i>	0.0396	M	1.26
1623065_at	<i>CG13692</i>	0.0396	M	1.52
1637128_a_at	<i>CG33340</i>	0.0396	M	6.38
1637156_at	<i>CG14717</i>	0.0396	M	1.33
1625481_a_at	<i>retn</i>	0.0450	F	1.34
1629097_at	<i>kni</i>	0.0450	F	3.30
1632422_s_at	<i>CG12901</i>	0.0399	M	2.51
1625255_at	<i>CG11029</i>	0.0454	F	1.31
1625850_at	<i>odd</i>	0.0454	F	1.33
1640670_at	<i>btl</i>	0.0401	M	2.25
1622919_at	<i>TwdIV</i>	0.0401	M	1.80
1626896_at	<i>CG34437</i>	0.0455	F	1.29
1641232_s_at	<i>CG32706</i>	0.0401	M	1.99
1641648_at	<i>CG3939</i>	0.0455	F	1.41
1635199_at	<i>CG6014</i>	0.0401	M	1.50
1639694_s_at	<i>Arc1</i>	0.0455	F	1.48
1638132_at	<i>CG10184</i>	0.0460	F	2.22
1626179_s_at	<i>Hsp60C</i>	0.0404	M	2.35
1629128_at	<i>CG8701</i>	0.0404	M	6.23
1623601_at	<i>Amyrel</i>	0.0472	F	2.09
1628307_at	<i>CG32388</i>	0.0404	M	3.73
1640979_at	<i>CG1681</i>	0.0472	F	1.69
1630617_at	<i>kek2</i>	0.0406	M	2.39
1627093_at	<i>CG9284</i>	0.0412	M	12.23
1637012_at	<i>m2</i>	0.0483	F	1.56
1629333_at	<i>CG32683</i>	0.0487	F	1.32
1634350_at	<i>sob</i>	0.0487	F	1.53
1639605_at	<i>CG33993</i>	0.0488	F	1.54
1635937_at	<i>CG4500</i>	0.0488	F	2.84
1636048_at	<i>Dak1</i>	0.0425	M	1.32
1624490_s_at	<i>hb</i>	0.0425	M	2.83
1634450_a_at	<i>CG14681</i>	0.0488	F	1.36
1633479_a_at	<i>CG4270</i>	0.0425	M	1.54
1636210_at	<i>CG10191</i>	0.0425	M	1.49
1629240_at	<i>Mst84Dc</i>	0.0426	M	17.72
1633396_at	<i>btd</i>	0.0493	F	1.54
1630503_at	<i>CG6045</i>	0.0432	M	1.69
1628593_at	<i>CG33252</i>	0.0432	M	1.57
1627838_at	<i>uzip</i>	0.0432	M	1.50
1637274_at	<i>CG14488</i>	0.0433	M	3.79
1625671_at	<i>lectin-37Db</i>	0.0504	F	1.15
1637211_at	<i>CG13045</i>	0.0434	M	1.46
1628962_at	<i>CG12708</i>	0.0434	M	1.54
1639634_at	<i>CG12860</i>	0.0434	M	3.01
1631780_at	<i>C15</i>	0.0440	M	1.67
1636376_at	<i>CG14947</i>	0.0440	M	1.73
163524_s_at	<i>CG32063</i>	0.0440	M	7.53
1635210_a_at	<i>Ppn</i>	0.0440	M	1.65
1640844_s_at	<i>Six4</i>	0.0440	M	1.81
1633989_at	<i>CG1124</i>	0.0440	M	1.72
1640096_at	<i>Fancd2</i>	0.0441	M	1.49
1631128_s_at	<i>CG9016</i>	0.0447	M	10.25
1627985_a_at	<i>CG31870</i>	0.0447	M	7.86
1640297_at	<i>CG31294</i>	0.0447	M	2.41
1634468_at	<i>CG13397</i>	0.0450	M	1.80
1639074_at	<i>CG33275</i>	0.0451	M	1.65

1633858_at	<i>CG4286</i>	0.0454	M	1.66
1637467_at	<i>CG5245</i>	0.0454	M	1.49
1627720_at	<i>CG14301</i>	0.0460	M	2.77
1626641_s_at	<i>glob1</i>	0.0472	M	1.71
1633070_at	<i>CG30222</i>	0.0483	M	1.45
1625981_at	<i>rab3-GEF</i>	0.0483	M	1.90
1633212_s_at	<i>CG31226</i>	0.0483	M	23.86
1640738_a_at	<i>spn-A</i>	0.0487	M	1.38
1625562_at	<i>CG34168</i>	0.0488	M	3.44
1636172_at	<i>CG12699</i>	0.0488	M	14.01
1630247_at	<i>CG4554</i>	0.0488	M	1.25
1626292_at	<i>CG4439</i>	0.0490	M	4.43
1631025_at	<i>Prosbeta5R1</i>	0.0490	M	1.17
1630663_a_at	<i>CG15219</i>	0.0493	M	11.73
1628570_at	<i>CG4021</i>	0.0493	M	1.97
1623539_at	<i>CG30039</i>	0.0493	M	7.98
1630158_at	<i>CG30429</i>	0.0493	M	2.07
1625606_at	<i>Ocho</i>	0.0493	M	1.78
1630009_at	<i>CG12209</i>	0.0494	M	1.26
1624711_at	<i>CG31740</i>	0.0494	M	5.84
1628672_at	<i>pio</i>	0.0494	M	1.14
1641024_at	<i>Hmr</i>	0.0494	M	1.30

*Affymetrix probe set ID.

[†]Annotated gene corresponding to probe set [if blank (-), the probe set maps to an unannotated region of the genome].

[‡]The lowest FDR threshold at which the probe set is called significant by SAM.

Table S4. Genes sex-differentially expressed at P20

Probe set*	Gene ^t	q-value [‡]	Sex bias	Fold difference
1633299_at	<i>lz</i>	0.0217	F	142.34
1623776_s_at	<i>dsx</i>	0.0217	F	28.31
1638037_a_at	<i>dpr17</i>	0.0217	F	17.79
1639734_at	<i>CG4017</i>	0.0217	M	13.41
1632742_at	<i>eyg</i>	0.0217	F	13.99
1632977_at	<i>Poxn</i>	0.0217	M	18.96
1634648_at	<i>Cpr47Ec</i>	0.0217	M	6.63
1639838_at	<i>CG8483</i>	0.0217	M	7.84
1623284_at	<i>CG10251</i>	0.0217	M	12.13
1633291_at	<i>dy</i>	0.0239	F	7.73
1631783_at	<i>CG4267</i>	0.0239	F	15.80
1636393_at	<i>CG15005</i>	0.0239	M	6.51
1635524_at	<i>CG30427</i>	0.0239	M	8.94
1629326_s_at	<i>eg</i>	0.0239	F	29.13
1640030_at	<i>CG4168</i>	0.0239	M	7.30
1633530_at	<i>HGTX</i>	0.0239	M	5.35
1637311_at	<i>pburs</i>	0.0239	M	8.71
1640844_s_at	<i>Six4</i>	0.0239	M	4.10
1627734_at	<i>nau</i>	0.0257	F	7.27
1638869_at	<i>Cpr51A</i>	0.0239	M	3.18
1633426_at	<i>Cpr78Cb</i>	0.0239	M	6.68
1635686_at	<i>CG14110</i>	0.0239	M	10.49
1627499_at	<i>CG2016</i>	0.0262	F	4.93
1622994_at	—	0.0241	M	9.58
1625321_a_at	<i>CG7549</i>	0.0262	F	2.68
1632431_s_at	<i>Ance</i>	0.0243	M	4.54
1636759_at	<i>CG8303</i>	0.0257	M	5.70
1633383_at	<i>toe</i>	0.0262	F	14.15
1629314_at	<i>CG12997</i>	0.0262	M	6.27
1630635_s_at	<i>CG7720</i>	0.0262	M	2.36
1641263_at	<i>CG31816</i>	0.0262	F	7.91
1622975_at	<i>CG13477</i>	0.0262	M	8.89
1635768_at	<i>CG4670</i>	0.0262	F	2.21
1633344_at	<i>Cpr92F</i>	0.0262	M	4.32
1637031_at	<i>gsb-n</i>	0.0262	M	4.89
1640697_at	—	0.0262	M	2.82
1624802_at	<i>CG31686</i>	0.0262	F	5.49
1626235_at	<i>m</i>	0.0262	M	4.76
1633879_a_at	<i>prd</i>	0.0262	M	7.99
1640494_at	<i>CG13272</i>	0.0262	F	2.47
1623206_a_at	<i>eya</i>	0.0262	M	3.61
1634113_at	<i>gk</i>	0.0262	M	4.40
1627096_s_at	<i>Tkr</i>	0.0262	F	14.49
1631774_at	<i>Cpr66Cb</i>	0.0262	F	5.61
1639545_a_at	<i>Awh</i>	0.0262	F	3.23
1632428_at	<i>CG11345</i>	0.0262	M	9.04
1639333_at	<i>al</i>	0.0262	F	3.34
1631400_at	<i>Cpr66D</i>	0.0262	M	10.98
1639042_at	<i>CG6414</i>	0.0262	M	4.44
1633377_at	<i>CG40303</i>	0.0262	M	6.44
1638896_at	<i>Cpr62Bc</i>	0.0262	F	9.74
1641137_at	<i>Dr</i>	0.0262	M	15.76
1623503_at	<i>sda</i>	0.0262	M	3.59
1637438_at	<i>Wnt2</i>	0.0262	M	2.87

1639473_at	<i>CG12541</i>	0.0262	F	2.41
1631128_s_at	<i>CG9016</i>	0.0262	M	4.99
1637658_at	<i>mth13</i>	0.0262	F	3.22
1637813_at	<i>abd-A</i>	0.0262	F	3.75
1633285_at	<i>y</i>	0.0262	M	3.76
1637211_at	<i>CG13045</i>	0.0262	M	3.71
1626388_at	<i>Ctr1B</i>	0.0262	M	5.41
1628256_at	<i>Mst77F</i>	0.0262	M	14.81
1631372_a_at	<i>AP-2</i>	0.0262	M	8.48
1627967_a_at	<i>mth14</i>	0.0268	F	2.93
1632860_at	<i>Cpr64Aa</i>	0.0262	M	5.93
1623983_at	<i>CG9514</i>	0.0262	M	8.45
1631262_at	<i>CG14866</i>	0.0262	M	7.84
1636772_s_at	<i>CG32694</i>	0.0262	M	4.45
1623466_at	<i>bab1</i>	0.0268	F	4.40
1622974_at	<i>CG4000</i>	0.0262	M	3.27
1636364_a_at	<i>CG17376</i>	0.0262	M	15.74
1637635_at	<i>CG4766</i>	0.0262	M	2.51
1629240_at	<i>Mst84Dc</i>	0.0262	M	25.02
1632591_at	<i>Phk-3</i>	0.0262	M	4.09
1636558_a_at	<i>abd-A</i>	0.0268	F	3.27
1639776_s_at	<i>CG1499</i>	0.0268	M	3.08
1630038_at	<i>pyd3</i>	0.0268	F	2.50
1634644_at	<i>CG42523</i>	0.0268	M	7.15
1625341_at	<i>FucTC</i>	0.0268	M	5.55
1636035_at	<i>beat-IIa</i>	0.0268	F	3.17
1638596_at	<i>ac</i>	0.0268	M	2.81
1633217_at	<i>CG30101</i>	0.0268	F	3.54
1627881_at	<i>salm</i>	0.0268	M	3.23
1641068_a_at	<i>spz</i>	0.0268	F	3.67
1624438_at	<i>CG5017</i>	0.0268	M	3.91
1631222_at	<i>pdm3</i>	0.0268	M	2.21
1626874_at	<i>Eip63F-1</i>	0.0268	F	17.03
1624374_at	<i>CG12481</i>	0.0268	M	5.90
1638277_at	<i>CG11550</i>	0.0268	M	2.47
1633031_at	<i>CG8299</i>	0.0268	M	3.32
1640129_at	<i>slp1</i>	0.0268	M	3.87
1629128_at	<i>CG8701</i>	0.0268	M	3.41
1629166_at	<i>sick</i>	0.0268	F	3.02
1637562_at	<i>TwdlT</i>	0.0268	F	5.78
1641282_at	<i>mth14</i>	0.0268	F	3.82
1625123_at	<i>CG2962</i>	0.0268	F	3.01
1639466_s_at	<i>CG30101</i>	0.0268	F	5.00
1636915_at	<i>CG11380</i>	0.0268	F	2.66
1636172_at	<i>CG12699</i>	0.0268	M	7.28
1633212_s_at	<i>CG31226</i>	0.0268	M	19.43
1628993_at	<i>beat-IIb</i>	0.0268	F	2.07
1625388_at	<i>CG4893</i>	0.0268	M	2.58
1624942_at	<i>bab1</i>	0.0268	F	3.00
1625273_at	<i>sc</i>	0.0268	M	2.52
1624460_s_at	<i>CG31988</i>	0.0268	M	2.69
1636404_at	<i>Mst35Bb</i>	0.0268	M	3.02
1631349_s_at	<i>tabor transposon</i>	0.0268	F	4.42
1635327_at	<i>CG31206</i>	0.0268	M	4.01
1634719_at	<i>CG9920</i>	0.0268	M	6.36
1624060_at	<i>bab2</i>	0.0268	F	2.45
1636387_at	<i>CG10300</i>	0.0268	F	2.88

1633827_at	<i>CG14327</i>	0.0268	M	5.51
1637639_at	<i>gsb</i>	0.0268	M	3.18
1624932_at	<i>Obp49a</i>	0.0268	M	4.41
1624175_at	<i>caup</i>	0.0268	M	3.17
1639559_at	<i>CG6431</i>	0.0268	F	6.03
1625620_a_at	<i>Sxl</i>	0.0268	F	3.18
1624490_s_at	<i>hb</i>	0.0268	M	3.09
1639110_at	<i>CG4484</i>	0.0268	M	4.98
1631714_a_at	<i>SP71</i>	0.0268	F	3.19
1641236_s_at	<i>CG5758</i>	0.0268	F	2.51
1626793_at	<i>CG30427</i>	0.0268	M	4.76
1629458_at	<i>CG9411</i>	0.0268	F	4.16
1628990_at	<i>Hmgcr</i>	0.0268	M	1.83
1637788_at	<i>CG31176</i>	0.0268	M	2.55
1636057_at	<i>CG9572</i>	0.0268	F	2.03
1625915_at	<i>CG4375</i>	0.0268	M	2.25
1635782_at	<i>CG32694</i>	0.0268	M	3.64
1627548_at	<i>CG12541</i>	0.0268	F	2.35
1626806_at	<i>tra</i>	0.0268	F	1.75
1634126_at	<i>CG31788</i>	0.0268	M	4.14
1637441_at	<i>CG3982</i>	0.0268	M	3.48
1633930_at	<i>CG1394</i>	0.0268	M	2.24
1639723_at	<i>CG7443</i>	0.0268	M	2.42
1629670_at	<i>CG17376</i>	0.0268	M	10.10
1630308_at	<i>CG3726</i>	0.0268	F	2.72
1638626_a_at	<i>os</i>	0.0268	M	4.79
1627053_at	<i>slp2</i>	0.0268	M	3.45
1640181_at	<i>CG13044</i>	0.0268	F	4.61
1624245_at	<i>CG15239</i>	0.0268	F	2.74
1640525_a_at	<i>CG15109</i>	0.0268	M	2.11
1637080_at	<i>CG9129</i>	0.0268	M	1.90
1634772_at	<i>CG1288</i>	0.0268	M	3.17
1636135_at	<i>CG13931</i>	0.0268	M	2.23
1632019_s_at	<i>CG9008</i>	0.0268	F	2.66
1624855_at	<i>CG31988</i>	0.0268	M	3.93
1628301_at	<i>CG32159</i>	0.0268	F	5.25
1630097_s_at	<i>CG17834</i>	0.0268	M	1.94
1625935_at	<i>Trim9</i>	0.0268	M	2.41
1624432_at	<i>Spz3</i>	0.0268	M	1.62
1639830_s_at	<i>CG8850</i>	0.0268	M	2.05
1635407_at	<i>CG32772</i>	0.0268	M	1.51
1634339_at	<i>CG32694</i>	0.0268	M	4.33
1631650_a_at	<i>spirit</i>	0.0268	M	1.80
1629120_at	<i>alpha-Man-l</i>	0.0268	M	2.33
1636376_at	<i>CG14947</i>	0.0268	M	2.04
1624990_at	<i>CG12063</i>	0.0268	M	2.77
1627120_at	<i>robl62A</i>	0.0268	M	3.72
1631211_at	<i>CG13245</i>	0.0268	M	2.07
1624503_at	<i>CG4786</i>	0.0278	F	2.44
1635374_at	<i>CG31728</i>	0.0268	M	2.21
1624444_at	<i>Mst84Da</i>	0.0268	M	5.97
1633776_s_at	<i>Mst35Ba</i>	0.0268	M	3.64
1634526_a_at	<i>qua</i>	0.0268	M	4.08
1625609_at	<i>CG32450</i>	0.0268	M	4.00
1626059_at	<i>knrl</i>	0.0279	F	2.26
1636835_at	<i>CG16700</i>	0.0268	M	2.49
1639741_at	<i>HLHm5</i>	0.0268	M	3.61

1637128_a_at	<i>CG33340</i>	0.0268	M	3.81
1631027_at	<i>ara</i>	0.0268	M	4.22
1632993_at	<i>CG6372</i>	0.0268	M	4.92
1636407_at	<i>gol</i>	0.0268	M	1.95
1629346_at	<i>CG1443</i>	0.0268	M	2.19
1624746_at	<i>betaTub85D</i>	0.0269	M	3.43
1635886_s_at	<i>blood transposon</i>	0.0284	F	2.02
1630663_a_at	<i>CG15219</i>	0.0278	M	4.69
1623004_a_at	<i>CG18449</i>	0.0279	M	3.56
1636879_at	<i>CG14356</i>	0.0279	M	3.30
1641527_at	<i>CG4576</i>	0.0279	M	1.89
1638512_at	<i>Sb</i>	0.0279	M	1.74
1624724_at	<i>b6</i>	0.0279	M	3.03
1639074_at	<i>CG33275</i>	0.0279	M	1.89
1641423_at	<i>CG6739</i>	0.0279	M	2.44
1625606_at	<i>Ocho</i>	0.0279	M	2.07
1628067_s_at	<i>dyl</i>	0.0279	M	3.99
1628878_at	<i>al</i>	0.0295	F	3.55
1635389_s_at	<i>Idgf4</i>	0.0279	M	2.16
1633305_at	<i>Obp99a</i>	0.0279	M	9.71
1641476_a_at	<i>Timp</i>	0.0279	M	2.26
1623707_a_at	<i>CG32192</i>	0.0279	M	2.71
1629097_at	<i>kni</i>	0.0295	F	2.47
1625625_at	<i>ImpE1</i>	0.0295	F	2.70
1624562_s_at	<i>Mst33A</i>	0.0279	M	2.20
1634880_s_at	<i>CG12902</i>	0.0279	M	5.04
1635163_at	<i>CG5731</i>	0.0279	M	1.82
1639425_at	<i>CG18662</i>	0.0279	M	7.52
1636473_at	<i>CG12861</i>	0.0279	M	3.54
1624456_at	<i>CG17154</i>	0.0280	M	1.98
1629263_at	<i>CG13699</i>	0.0284	M	1.95
1624819_s_at	<i>gypsy transposon</i>	0.0298	F	3.26
1641074_s_at	<i>Myo31DF</i>	0.0284	M	1.87
1631816_at	<i>Akh</i>	0.0284	M	3.65
1622919_at	<i>TwdIV</i>	0.0284	M	2.41
1637225_at	<i>bnl</i>	0.0284	M	2.05
1627093_at	<i>CG9284</i>	0.0284	M	10.75
1628334_at	<i>m4</i>	0.0284	M	3.08
1623395_at	-	0.0284	M	2.62
1632353_at	<i>CG7884</i>	0.0284	M	1.48
1640057_at	<i>CG9192</i>	0.0302	F	3.08
1629893_s_at	<i>transposon</i>	0.0302	F	1.94
1633977_at	<i>CG42735</i>	0.0302	F	2.29
1632781_s_at	<i>Abd-B</i>	0.0287	M	1.73
1635194_at	<i>CG13869</i>	0.0287	M	3.46
1632422_s_at	<i>CG12901</i>	0.0295	M	1.97
1626031_at	<i>CG12539</i>	0.0295	M	2.11
1635124_at	<i>ase</i>	0.0295	M	2.50
1632082_at	<i>Ndg</i>	0.0295	M	2.27
1640034_at	<i>CG13110</i>	0.0295	M	2.57
1635092_at	<i>CG33557</i>	0.0295	M	4.92
1638494_at	<i>CG3124</i>	0.0295	M	2.94
1632254_a_at	<i>CG30270</i>	0.0295	M	5.69
1628450_at	<i>Nplp1</i>	0.0295	M	2.04
1638428_at	<i>TART-element transposon</i>	0.0295	M	10.70
1640487_at	<i>CG12689</i>	0.0295	M	3.48
1624069_at	<i>CG7296</i>	0.0319	F	1.74

1638458_at	<i>ImpE1</i>	0.0319	F	2.05
1623601_at	<i>Amyrel</i>	0.0295	M	2.02
1639413_at	<i>ocn</i>	0.0295	M	15.13
1626854_at	<i>CG32148</i>	0.0295	M	1.81
1639431_at	<i>synaptogyrin</i>	0.0295	M	2.35
1629776_a_at	<i>CG6643</i>	0.0295	M	1.85
1639535_at	<i>pgant2</i>	0.0295	M	1.56
1630670_at	<i>CG1368</i>	0.0295	M	1.84
1624517_at	<i>Ect3</i>	0.0324	F	2.36
1635267_s_at	<i>Tsp66E</i>	0.0295	M	1.34
1623539_at	<i>CG30039</i>	0.0298	M	6.81
1626133_s_at	<i>transposon</i>	0.0327	F	2.07
1637851_at	<i>CG7422</i>	0.0327	F	1.81
1629812_at	<i>CG14915</i>	0.0298	M	3.01
1640348_at	<i>CG5050</i>	0.0298	M	2.27
1637037_at	<i>ade3</i>	0.0298	M	1.66
1623558_at	<i>Cpr49Ae</i>	0.0298	M	2.46
1637867_at	<i>mid</i>	0.0298	M	1.55
1625207_at	<i>CG32636</i>	0.0331	F	2.91
1625454_at	<i>Gbeta5</i>	0.0298	M	2.16
1626048_at	<i>HLHmgamma</i>	0.0298	M	2.08
1639732_s_at	<i>salr</i>	0.0298	M	2.03
1635411_at	<i>CG32652</i>	0.0298	M	2.70
1624916_a_at	<i>CG33293</i>	0.0298	M	2.35
1636668_at	<i>CG9972</i>	0.0298	M	1.74
1627432_at	<i>CG6041</i>	0.0298	M	1.78
1624556_s_at	<i>bol</i>	0.0302	M	2.02
1629116_at	<i>CG14545</i>	0.0302	M	2.35
1629780_at	<i>CG13471</i>	0.0305	M	1.97
1624989_s_at	<i>Ef1alpha100E</i>	0.0356	F	1.56
1638582_at	<i>CG5321</i>	0.0356	F	2.10
1628584_at	<i>Cyp305a1</i>	0.0309	M	1.80
1633704_at	<i>CG7045</i>	0.0309	M	3.08
1637600_at	<i>CG14926</i>	0.0309	M	6.48
1639483_s_at	<i>Nep1</i>	0.0309	M	2.15
1641512_at	<i>CG15473</i>	0.0309	M	2.48
1641259_at	<i>Chit</i>	0.0365	F	2.97
1636905_at	<i>lea</i>	0.0309	M	1.95
1633429_at	<i>mof</i>	0.0310	M	1.59
1628348_at	<i>CG32081</i>	0.0310	M	2.38
1633068_at	<i>loopin-1</i>	0.0310	M	1.63
1627719_at	<i>gol</i>	0.0310	M	1.80
1635007_at	<i>Sulf1</i>	0.0319	M	1.51
1623634_at	<i>CG6527</i>	0.0319	M	2.07
1634842_a_at	<i>CG11160</i>	0.0377	F	1.71
1630102_at	<i>CG12617</i>	0.0320	M	2.76
1633264_at	<i>CG13024</i>	0.0378	F	2.71
1628779_a_at	<i>svp</i>	0.0321	M	2.80
1623624_at	<i>CG14869</i>	0.0321	M	1.68
1640759_at	<i>CG31709</i>	0.0321	M	2.71
1640837_a_at	<i>ImpL1</i>	0.0321	M	1.73
1632294_at	<i>sens</i>	0.0321	M	2.42
1631252_a_at	<i>GV1</i>	0.0387	F	1.66
1640950_at	<i>CG15739</i>	0.0321	M	1.84
1628414_at	<i>CG4955</i>	0.0321	M	2.27
1639372_s_at	<i>CG17567</i>	0.0321	M	4.72
1632367_at	<i>Mst35Ba</i>	0.0321	M	2.33

1623980_at	<i>CG15905</i>	0.0392	F	1.83
1626536_at	<i>CG6776</i>	0.0324	M	2.03
1623096_a_at	<i>Tsp68C</i>	0.0324	M	2.27
1638296_at	<i>CG32064</i>	0.0324	M	2.93
1637805_at	<i>pdm3</i>	0.0324	M	2.54
1635086_at	<i>CG4666</i>	0.0324	M	2.35
1628412_at	<i>Ac78C</i>	0.0324	M	6.64
1634063_a_at	<i>stumps</i>	0.0324	M	1.71
1636646_at	<i>sna</i>	0.0324	M	1.88
1631436_at	<i>Mst98Cb</i>	0.0327	M	2.04
1635896_at	-	0.0409	F	1.38
1632533_at	<i>Timp</i>	0.0327	M	2.21
1630171_at	<i>Cpr97Ea</i>	0.0327	M	1.71
1625687_at	<i>kon</i>	0.0327	M	1.67
1639515_at	<i>CG7367</i>	0.0327	M	1.49
1623517_at	<i>CG4962</i>	0.0327	M	2.51
1634372_at	<i>Ddr</i>	0.0416	F	1.65
1630819_at	<i>CG7046</i>	0.0331	M	2.50
1633795_a_at	<i>CG17124</i>	0.0420	F	1.57
1625293_at	<i>CG14397</i>	0.0421	F	2.68
1624286_at	<i>janB</i>	0.0336	M	3.07
1633262_s_at	<i>Lim1</i>	0.0422	F	1.78
1626984_at	<i>Gld</i>	0.0422	F	2.32
1640607_at	<i>org-1</i>	0.0425	F	1.66
1635139_at	<i>CG13340</i>	0.0338	M	3.71
1627985_a_at	<i>CG31870</i>	0.0338	M	5.45
1635366_at	<i>CG5614</i>	0.0338	M	2.04
1629242_x_at	<i>TART-element transposon</i>	0.0338	M	4.80
1638195_at	<i>beltless</i>	0.0338	M	1.82
1641132_at	<i>CG30497</i>	0.0428	F	2.14
1631631_at	<i>Cpr47Ee</i>	0.0428	F	2.00
1623083_at	<i>CG1698</i>	0.0340	M	1.81
1627679_at	<i>CG12470</i>	0.0340	M	2.09
1632189_at	<i>CG3587</i>	0.0434	F	1.54
1641143_s_at	<i>tsl</i>	0.0434	F	1.49
1641366_at	<i>eIF4E-3</i>	0.0346	M	2.15
1630512_at	<i>CG8316</i>	0.0346	M	1.69
1631112_at	<i>Epac</i>	0.0356	M	2.69
1625279_a_at	<i>tup</i>	0.0356	M	1.80
1626241_at	<i>Cyt-c-d</i>	0.0357	M	1.59
1632430_at	<i>Tsf1</i>	0.0357	M	1.62
1639479_a_at	<i>kn</i>	0.0357	M	2.41
1624711_at	<i>CG31740</i>	0.0357	M	4.92
1640126_at	<i>CG8249</i>	0.0357	M	1.94
1627511_at	<i>chrb</i>	0.0453	F	1.35
1630883_at	<i>CG33978</i>	0.0357	M	1.56
1626011_at	<i>CG17834</i>	0.0357	M	1.56
1623465_at	<i>CG6138</i>	0.0357	M	1.63
1639827_at	<i>CG3581</i>	0.0357	M	1.54
1635835_at	<i>CG30374</i>	0.0453	F	2.25
1624982_s_at	<i>CG5080</i>	0.0453	F	1.55
1625245_at	<i>CG3759</i>	0.0458	F	1.77
1624408_at	<i>NetA</i>	0.0365	M	1.93
1638870_at	<i>CG1958</i>	0.0366	M	1.80
1641413_s_at	<i>CG3074</i>	0.0366	M	1.73
1635270_at	<i>CG33958</i>	0.0465	F	1.66
1633607_at	<i>CG2444</i>	0.0366	M	2.14

1625641_s_at	CG9650	0.0465	F	2.31
1630014_at	Nox	0.0465	F	1.95
1641418_at	CG2955	0.0367	M	1.48
1635900_at	Thor	0.0367	M	1.81
1640509_s_at	lama	0.0367	M	1.57
1630784_a_at	CG9990	0.0367	M	1.49
1630120_s_at	-	0.0474	F	3.46
1638899_s_at	CG15312	0.0474	F	1.52
1629944_at	CG12814	0.0372	M	1.71
1635424_s_at	CG32063	0.0377	M	5.44
1629227_at	baz	0.0377	M	1.40
1631498_a_at	fru	0.0477	F	2.37
1632966_at	CG8213	0.0378	M	1.89
1640799_at	dsx	0.0378	M	1.79
1625562_at	CG34168	0.0378	M	2.05
1629693_at	CG15080	0.0489	F	1.79
1630142_at	sog	0.0489	F	1.84
1630064_at	CG5639	0.0381	M	2.14
1639229_at	vkg	0.0489	F	1.96
1641727_at	CG17470	0.0381	M	2.41
1630969_s_at	CG12206	0.0489	F	1.70
1631125_at	CG15737	0.0381	M	1.45
1628383_at	CG3330	0.0381	M	1.99
1626910_at	CG15282	0.0382	M	5.46
1629011_at	TwdlN	0.0384	M	1.99
1626846_s_at	CG5973	0.0387	M	1.59
1639152_at	Ptp52F	0.0387	M	2.31
1637812_at	CG30430	0.0387	M	3.92
1631394_at	CG31324	0.0387	M	2.25
1635987_at	CG12116	0.0512	F	3.28
1638262_at	CG17819	0.0392	M	2.32
1625947_at	GLaz	0.0394	M	1.41
1629966_at	E(spl)	0.0396	M	1.94
1627342_at	CG15251	0.0396	M	1.59
1624850_at	CG3556	0.0396	M	1.61
1623372_at	CG5873	0.0398	M	1.39
1627875_at	CG12814	0.0409	M	1.81
1639779_at	CG17376	0.0416	M	3.29
1628307_at	CG32388	0.0420	M	2.13
1624403_at	CG13071	0.0420	M	1.59
1638603_at	CG31909	0.0420	M	2.00
1634261_at	Cyp312a1	0.0420	M	1.83
1632680_at	Pgant35A	0.0421	M	1.48
1630577_at	CG17378	0.0422	M	1.40
1640327_at	CG6023	0.0422	M	2.03
1640160_a_at	CG31948	0.0422	M	1.94
1633080_at	CG14835	0.0423	M	1.89
1633574_at	CG31820	0.0425	M	4.43
1634667_at	CG11099	0.0425	M	2.39
1624839_at	h	0.0425	M	1.44
1639218_s_at	CG15530	0.0425	M	1.56
1629303_at	CG32832	0.0427	M	4.01
1635840_s_at	msl-2	0.0427	M	1.97
1623569_at	CG14906	0.0429	M	1.63
1641535_at	CG9555	0.0430	M	1.74
1629914_at	CG34281	0.0430	M	1.57
1626572_at	CG10822	0.0434	M	1.65

1633524_a_at	<i>CalpA</i>	0.0434	M	1.32
1630255_at	<i>CG31676</i>	0.0437	M	1.65
1623770_at	<i>CG1673</i>	0.0439	M	2.53
1639539_at	<i>Cyp4e1</i>	0.0441	M	1.82
1638810_at	<i>Faa</i>	0.0442	M	2.05
1634597_a_at	<i>CG33970</i>	0.0453	M	1.27
1626470_at	<i>CG10440</i>	0.0453	M	1.67
1633869_at	<i>Dfd</i>	0.0453	M	1.85
1624525_at	<i>CG12998</i>	0.0454	M	3.40
1634777_at	<i>CG13297</i>	0.0458	M	1.48
1630075_s_at	<i>sep4</i>	0.0458	M	1.78
1629206_at	-	0.0458	M	1.37
1637078_a_at	<i>Poxm</i>	0.0460	M	1.62
1637495_at	<i>CG18735</i>	0.0465	M	1.67
1623935_at	<i>sxe2</i>	0.0465	M	1.84
1631725_at	<i>CG4691</i>	0.0470	M	1.63
1631991_at	<i>CG5089</i>	0.0470	M	1.84
1637306_at	<i>CG31720</i>	0.0470	M	1.93
1631157_at	<i>CG7365</i>	0.0474	M	1.64
1636988_at	<i>CG8476</i>	0.0474	M	2.81
1624202_a_at	<i>CG2127</i>	0.0474	M	1.65
1623978_at	<i>CG10862</i>	0.0474	M	1.73
1631300_at	<i>Cyp18a1</i>	0.0474	M	1.83
1629233_s_at	<i>CG16708</i>	0.0474	M	1.28
1639575_at	<i>CG18446</i>	0.0474	M	1.55
1628874_at	<i>CG15200</i>	0.0474	M	2.02
1624433_at	<i>CG10589</i>	0.0474	M	1.50
1624412_at	<i>ap</i>	0.0474	M	2.00
1637228_at	<i>CG10663</i>	0.0477	M	1.43
1634166_at	<i>lea</i>	0.0479	M	1.53
1627235_at	<i>CG17207</i>	0.0479	M	1.52
1627445_s_at	<i>en</i>	0.0479	M	1.54
1623813_at	<i>CG33307</i>	0.0480	M	2.40
1636998_at	<i>sca</i>	0.0480	M	2.12
1634198_at	<i>beltless</i>	0.0489	M	1.86
1626457_s_at	<i>CG31163</i>	0.0490	M	1.57
1633000_a_at	<i>CadN</i>	0.0492	M	1.35
1626594_s_at	<i>svp</i>	0.0495	M	2.17
1632706_at	<i>CG13054</i>	0.0499	M	2.31

*Affymetrix probe set ID.

[†]Annotated gene corresponding to probe set [if blank (-), the probe set maps to an unannotated region of the genome].

[‡]The lowest FDR threshold at which the probe set is called significant by SAM.

Table S5. Gene expression clusters defined by PAM

Cluster*	Probe set [†]	Gene [‡]
1	1641137_at	<i>Dr</i>
1	1639483_s_at	<i>Nep1</i>
1	1637225_at	<i>bnl</i>
1	1633377_at	—
1	1631372_a_at	<i>AP-2</i>
1	1626388_at	<i>Ctr1B</i>
1	1625341_at	<i>FucTC</i>
1	1624175_at	<i>caup</i>
1	1639433_at	<i>dpn</i>
1	1627135_at	<i>bnl</i>
1	1636668_at	<i>CG9972</i>
1	1627053_at	<i>slp2</i>
1	1625535_at	<i>H15</i>
1	1640799_at	<i>dsx</i>
1	1633530_at	<i>HGTX</i>
1	1632431_s_at	<i>Ance</i>
1	1631027_at	<i>ara</i>
1	1627881_at	<i>salm</i>
1	1627445_s_at	<i>en</i>
1	1627432_at	<i>CG6041</i>
1	1623395_at	—
1	1623206_a_at	<i>eya</i>
1	1641219_at	<i>CG11136</i>
1	1639868_at	<i>CG1702</i>
1	1638907_at	<i>msi</i>
1	1638821_a_at	<i>yuri</i>
1	1638186_a_at	<i>Fem-1</i>
1	1637467_at	<i>CG5245</i>
1	1637049_at	<i>bi</i>
1	1637021_at	<i>stumps</i>
1	1636969_at	<i>Poxm</i>
1	1636536_at	<i>Pglym87</i>
1	1634873_at	<i>stumps</i>
1	1631780_at	<i>C15</i>
1	1631077_at	<i>CG16957</i>
1	1625844_s_at	<i>apt</i>
1	1624624_at	<i>mud</i>
1	1624543_s_at	<i>springer transposon</i>
1	1641074_s_at	<i>Myo31DF</i>
1	1640126_at	<i>CG8249</i>
1	1638428_at	<i>TART-element transposon</i>
1	1637037_at	<i>ade3</i>
1	1633429_at	<i>mof</i>
1	1630512_at	<i>CG8316</i>
1	1629242_x_at	<i>TART-element transposon</i>
1	1628414_at	<i>CG4955</i>
1	1624456_at	<i>CG17154</i>
1	1624286_at	<i>janB</i>
1	1623935_at	<i>sxe2</i>
2	1640697_at	—
2	1637438_at	<i>Wnt2</i>
2	1639723_at	<i>CG7443</i>
2	1639425_at	<i>CG18662</i>
2	1637311_at	<i>pburs</i>
2	1637128_a_at	<i>CG33340</i>
2	1637078_a_at	<i>Poxm</i>
2	1636759_at	<i>CG8303</i>
2	1636646_at	<i>sna</i>
2	1636364_a_at	<i>CG17376</i>
2	1636172_at	<i>CG12699</i>
2	1635424_s_at	<i>CG32063</i>
2	1635139_at	<i>CG13340</i>
2	1634644_at	<i>CG42523</i>
2	1634126_at	<i>CG31788</i>
2	1633212_s_at	<i>CG31226</i>
2	1632993_at	<i>CG6372</i>
2	1632422_s_at	<i>CG12901</i>
2	1631394_at	<i>CG31324</i>
2	1631128_s_at	<i>CG9016</i>
2	1630663_a_at	<i>CG15219</i>
2	1629670_at	<i>CG17376</i>
2	1629240_at	<i>Mst84Dc</i>

2	1629128_at	<i>CG8701</i>
2	1628584_at	<i>Cyp305a1</i>
2	1628307_at	<i>CG32388</i>
2	1627985_a_at	<i>CG31870</i>
2	1627093_at	<i>CG9284</i>
2	1626241_at	<i>Cyt-c-d</i>
2	1625562_at	<i>CG34168</i>
2	1624711_at	<i>CG31740</i>
2	1623978_at	<i>CG10862</i>
2	1623539_at	<i>CG30039</i>
2	1640297_at	<i>CG31294</i>
2	1639634_at	<i>CG12860</i>
2	1639165_at	<i>Mst84Dd</i>
2	1638853_at	<i>CG32971</i>
2	1638441_a_at	<i>CG18519</i>
2	1638284_at	<i>CG3199</i>
2	1637790_a_at	<i>CG12250</i>
2	1637274_at	<i>CG14488</i>
2	1636742_at	<i>nord</i>
2	1634778_at	<i>CG3092</i>
2	1633748_at	<i>CG2014</i>
2	1633591_at	<i>gcm2</i>
2	1633479_a_at	<i>CG4270</i>
2	1633070_at	<i>CG30222</i>
2	1632039_at	<i>CG4546</i>
2	1631346_a_at	<i>CG30412</i>
2	1631238_at	<i>Hsp60B</i>
2	1631126_at	<i>gcm</i>
2	1630337_at	<i>CG15927</i>
2	1630158_at	<i>CG30429</i>
2	1628570_at	<i>CG4021</i>
2	1628089_at	<i>ham</i>
2	1626292_at	<i>CG4439</i>
2	1626179_s_at	<i>Hsp60C</i>
2	1625913_at	<i>CG9970</i>
2	1625510_at	<i>Osi1</i>
2	1624229_at	<i>CG15705</i>
2	1641727_at	<i>CG17470</i>
2	1641418_at	<i>CG2955</i>
2	1641366_at	<i>eIF4E-3</i>
2	1640759_at	<i>CG31709</i>
2	1640525_a_at	<i>CG15109</i>
2	1640487_at	<i>CG12689</i>
2	1640348_at	<i>CG5050</i>
2	1640160_a_at	<i>CG31948</i>
2	1640034_at	<i>CG13110</i>
2	1639827_at	<i>CG3581</i>
2	1639779_at	<i>CG17376</i>
2	1639413_at	<i>ocn</i>
2	1639372_s_at	<i>CG17567</i>
2	1639218_s_at	<i>CG15530</i>
2	1638870_at	<i>CG1958</i>
2	1638626_a_at	<i>os</i>
2	1638603_at	<i>CG31909</i>
2	1638494_at	<i>CG3124</i>
2	1638296_at	<i>CG32064</i>
2	1638262_at	<i>CG17819</i>
2	1637812_at	<i>CG30430</i>
2	1637600_at	<i>CG14926</i>
2	1637441_at	<i>CG3982</i>
2	1637080_at	<i>CG9129</i>
2	1636988_at	<i>CG8476</i>
2	1636473_at	<i>CG12861</i>
2	1636404_at	<i>Mst35Bb</i>
2	1635411_at	<i>CG32652</i>
2	1635366_at	<i>CG5614</i>
2	1635327_at	<i>CG31206</i>
2	1634880_s_at	<i>CG12902</i>
2	1634772_at	<i>CG1288</i>
2	1634719_at	<i>CG9920</i>
2	1633930_at	<i>CG1394</i>
2	1633776_s_at	<i>Mst35Ba</i>
2	1633704_at	<i>CG7045</i>
2	1633574_at	<i>CG31820</i>
2	1633068_at	<i>loopin-1</i>

2	1632367_at	<i>Mst35Ba</i>
2	1632254_a_at	<i>CG30270</i>
2	1631991_at	<i>CG5089</i>
2	1631725_at	<i>CG4691</i>
2	1631436_at	<i>Mst98Cb</i>
2	1631211_at	<i>CG13245</i>
2	1630819_at	<i>CG7046</i>
2	1630102_at	<i>CG12617</i>
2	1629780_at	<i>CG13471</i>
2	1629303_at	<i>CG32832</i>
2	1628874_at	<i>CG15200</i>
2	1628383_at	<i>CG3330</i>
2	1628348_at	<i>CG32081</i>
2	1628256_at	<i>Mst77F</i>
2	1627235_at	<i>CG17207</i>
2	1627120_at	<i>robl62A</i>
2	1626854_at	<i>CG32148</i>
2	1626572_at	<i>CG10822</i>
2	1625915_at	<i>CG4375</i>
2	1625609_at	<i>CG32450</i>
2	1624916_a_at	<i>CG33293</i>
2	1624855_at	<i>CG31988</i>
2	1624746_at	<i>betaTub85D</i>
2	1624562_s_at	<i>Mst33A</i>
2	1624556_s_at	<i>bol</i>
2	1624460_s_at	<i>CG31988</i>
2	1624444_at	<i>Mst84Da</i>
2	1624438_at	<i>CG5017</i>
2	1624202_a_at	<i>CG2127</i>
2	1623634_at	<i>CG6527</i>
2	1623465_at	<i>CG6138</i>
2	1623004_a_at	<i>CG18449</i>
2	1622975_at	<i>CG13477</i>
3	1626934_a_at	<i>wb</i>
3	1625940_s_at	<i>sim</i>
3	1636392_at	<i>CG15785</i>
3	1631471_at	<i>CG14889</i>
3	1636905_at	<i>lea</i>
3	1634526_a_at	<i>qua</i>
3	1634063_a_at	<i>stumps</i>
3	1641024_at	<i>Hmr</i>
3	1640738_a_at	<i>spn-A</i>
3	1640513_a_at	<i>CG32150</i>
3	1639636_at	<i>Cht7</i>
3	1638592_at	<i>CG6560</i>
3	1637156_at	<i>CG14717</i>
3	1634833_at	<i>PQBP-1</i>
3	1633623_s_at	<i>sano</i>
3	1633480_at	<i>CG5392</i>
3	1631323_a_at	<i>CG2663</i>
3	1630617_at	<i>kek2</i>
3	1628593_at	<i>CG33252</i>
3	1627971_s_at	<i>sano</i>
3	1640509_s_at	<i>lama</i>
3	1637228_at	<i>CG10663</i>
3	1636879_at	<i>CG14356</i>
3	1635407_at	<i>CG32772</i>
3	1635124_at	<i>ase</i>
3	1635007_at	<i>Sulf1</i>
3	1633000_a_at	<i>CadN</i>
3	1632680_at	<i>Pgant35A</i>
3	1632294_at	<i>sens</i>
3	1630075_s_at	<i>sep4</i>
3	1627719_at	<i>gol</i>
3	1626846_s_at	<i>CG5973</i>
3	1625947_at	<i>GLaz</i>
3	1624408_at	<i>NetA</i>
3	1623096_a_at	<i>Tsp68C</i>
3	1631252_a_at	<i>GV1</i>
4	1637635_at	<i>CG4766</i>
4	1639776_s_at	<i>CG1499</i>
4	1639741_at	<i>HLHm5</i>
4	1636393_at	<i>CG15005</i>
4	1632591_at	<i>Phk-3</i>
4	1626235_at	<i>m</i>

4	1625935_at	<i>Trim9</i>
4	1632781_s_at	<i>Abd-B</i>
4	1626892_at	<i>del</i>
4	1640950_at	<i>CG15739</i>
4	1639838_at	<i>CG8483</i>
4	1639515_at	<i>CG7367</i>
4	1637639_at	<i>gsb</i>
4	1637031_at	<i>gsb-n</i>
4	1635782_at	<i>CG32694</i>
4	1635686_at	<i>CG14110</i>
4	1635524_at	<i>CG30427</i>
4	1635267_s_at	<i>Tsp66E</i>
4	1634648_at	<i>Cpr47Ec</i>
4	1634339_at	<i>CG32694</i>
4	1634198_at	<i>beltless</i>
4	1633285_at	<i>y</i>
4	1631650_a_at	<i>spirit</i>
4	1631125_at	<i>CG15737</i>
4	1631112_at	<i>Epac</i>
4	1630883_at	<i>CG33978</i>
4	1630577_at	<i>CG17378</i>
4	1629944_at	<i>CG12814</i>
4	1629206_at	—
4	1627875_at	<i>CG12814</i>
4	1627679_at	<i>CG12470</i>
4	1626793_at	<i>CG30427</i>
4	1626457_s_at	<i>CG31163</i>
4	1626048_at	<i>HLHmgamma</i>
4	1624433_at	<i>CG10589</i>
4	1623569_at	<i>CG14906</i>
4	1623558_at	<i>Cpr49Ae</i>
4	1638596_at	<i>ac</i>
5	1639732_s_at	<i>salr</i>
5	1635840_s_at	<i>msl-2</i>
5	1632977_at	<i>Poxn</i>
5	1624412_at	<i>ap</i>
5	1640844_s_at	<i>Six4</i>
5	1639734_at	<i>CG4017</i>
5	1639074_at	<i>CG33275</i>
5	1636376_at	<i>CG14947</i>
5	1633879_a_at	<i>prd</i>
5	1629227_at	<i>baz</i>
5	1628450_at	<i>Nplp1</i>
5	1625606_at	<i>Ocho</i>
5	1625454_at	<i>Gbeta5</i>
5	1624932_at	<i>Obp49a</i>
5	1624490_s_at	<i>hb</i>
5	1623707_a_at	<i>CG32192</i>
5	1622919_at	<i>TwdIV</i>
5	1641232_s_at	<i>CG32706</i>
5	1640261_at	<i>CG9522</i>
5	1634211_at	<i>arr</i>
5	1631597_at	<i>foxo</i>
5	1630009_at	<i>CG12209</i>
5	1627838_at	<i>uzip</i>
5	1625727_at	<i>CG32006</i>
5	1624699_s_at	<i>Bx</i>
5	1641512_at	<i>CG15473</i>
5	1640030_at	<i>CG4168</i>
5	1639479_a_at	<i>kn</i>
5	1639110_at	<i>CG4484</i>
5	1638195_at	<i>beltless</i>
5	1636135_at	<i>CG13931</i>
5	1635194_at	<i>CG13869</i>
5	1635092_at	<i>CG33557</i>
5	1634777_at	<i>CG13297</i>
5	1634667_at	<i>CG11099</i>
5	1634166_at	<i>lea</i>
5	1633344_at	<i>Cpr92F</i>
5	1633080_at	<i>CG14835</i>
5	1633031_at	<i>CG8299</i>
5	1632860_at	<i>Cpr64Aa</i>
5	1631816_at	<i>Akh</i>
5	1630635_s_at	<i>CG7720</i>
5	1629346_at	<i>CG1443</i>

5	1629314_at	<i>CG12997</i>
5	1629116_at	<i>CG14545</i>
5	1628412_at	<i>Ac78C</i>
5	1625279_a_at	<i>tup</i>
5	1624850_at	<i>CG3556</i>
5	1623813_at	<i>CG33307</i>
5	1623284_at	<i>CG10251</i>
5	1622994_at	—
5	1622974_at	<i>CG4000</i>
6	1640670_at	<i>btl</i>
6	1640327_at	<i>CG6023</i>
6	1634261_at	<i>Cyp312a1</i>
6	1631222_at	<i>pdm3</i>
6	1630097_s_at	<i>CG17834</i>
6	1626470_at	<i>CG10440</i>
6	1623770_at	<i>CG1673</i>
6	1640097_at	<i>Pxn</i>
6	1638324_s_at	<i>CG6921</i>
6	1637246_a_at	<i>CG32627</i>
6	1634552_at	<i>TepIV</i>
6	1634468_at	<i>CG13397</i>
6	1630503_at	<i>CG6045</i>
6	1629365_at	<i>CG30324</i>
6	1628125_at	<i>Doc2</i>
6	1626570_s_at	<i>SNF4Agamma</i>
6	1626383_at	<i>CG4096</i>
6	1624813_s_at	<i>CG34008</i>
6	1623909_s_at	<i>inv</i>
6	1623092_at	<i>Pcp</i>
6	1623065_at	<i>CG13692</i>
6	1640129_at	<i>slp1</i>
6	1637805_at	<i>pdm3</i>
6	1637306_at	<i>CG31720</i>
6	1635389_s_at	<i>ldgf4</i>
6	1633607_at	<i>CG2444</i>
6	1626011_at	<i>CG17834</i>
6	1624839_at	<i>h</i>
7	1633305_at	<i>Obp99a</i>
7	1629120_at	<i>alpha-Man-I</i>
7	1641422_at	<i>htt</i>
7	1640096_at	<i>Fancd2</i>
7	1637513_at	<i>CG11275</i>
7	1636210_at	<i>CG10191</i>
7	1635210_a_at	<i>Ppn</i>
7	1633989_at	<i>CG1124</i>
7	1633341_s_at	<i>dac</i>
7	1633032_s_at	<i>CG8177</i>
7	1631408_at	<i>SoxN</i>
7	1631025_at	<i>Prosbeta5R1</i>
7	1629048_s_at	<i>CG9674</i>
7	1628774_a_at	<i>boi</i>
7	1628672_at	<i>pio</i>
7	1628604_at	<i>D</i>
7	1626773_s_at	<i>CG18431</i>
7	1624297_at	<i>drl</i>
7	1641527_at	<i>CG4576</i>
7	1639830_s_at	<i>CG8850</i>
7	1635374_at	<i>CG31728</i>
7	1635163_at	<i>CG5731</i>
7	1633426_at	<i>Cpr78Cb</i>
7	1632428_at	<i>CG11345</i>
7	1631157_at	<i>CG7365</i>
7	1630255_at	<i>CG31676</i>
7	1629812_at	<i>CG14915</i>
7	1629776_a_at	<i>CG6643</i>
7	1629233_s_at	<i>CG16708</i>
7	1626031_at	<i>CG12539</i>
7	1625388_at	<i>CG4893</i>
7	1624990_at	<i>CG12063</i>
7	1623624_at	<i>CG14869</i>
7	1623517_at	<i>CG4962</i>
7	1623980_at	<i>CG15905</i>
7	1625255_at	<i>CG11029</i>
7	1625198_at	<i>ss</i>
8	1632317_at	<i>CG3036</i>

8	1639535_at	<i>pgant2</i>
8	1626903_at	<i>CG3355</i>
8	1625621_s_at	<i>f</i>
8	1637211_at	<i>CG13045</i>
8	1638051_at	<i>CG17323</i>
8	1636688_at	<i>Cyp4s3</i>
8	1633952_at	<i>CG7080</i>
8	1630570_at	<i>CG13003</i>
8	1627720_at	<i>CG14301</i>
8	1627681_at	<i>Cpr35B</i>
8	1625981_at	<i>rab3-GEF</i>
8	1641423_at	<i>CG6739</i>
8	1640837_a_at	<i>ImpL1</i>
8	1639539_at	<i>Cyp4e1</i>
8	1638869_at	<i>Cpr51A</i>
8	1638512_at	<i>Sb</i>
8	1637788_at	<i>CG31176</i>
8	1636772_s_at	<i>CG32694</i>
8	1635086_at	<i>CG4666</i>
8	1634113_at	<i>gk</i>
8	1633827_at	<i>CG14327</i>
8	1632966_at	<i>CG8213</i>
8	1632353_at	<i>CG7884</i>
8	1631300_at	<i>Cyp18a1</i>
8	1631262_at	<i>CG14866</i>
8	1630784_a_at	<i>CG9990</i>
8	1630670_at	<i>CG1368</i>
8	1630064_at	<i>CG5639</i>
8	1629966_at	<i>E(spl)</i>
8	1629263_at	<i>CG13699</i>
8	1628990_at	<i>Hmgcr</i>
8	1628067_s_at	<i>dyl</i>
8	1627342_at	<i>CG15251</i>
8	1625273_at	<i>sc</i>
8	1624724_at	<i>b6</i>
8	1624432_at	<i>Spz3</i>
8	1624374_at	<i>CG12481</i>
8	1623983_at	<i>CG9514</i>
8	1623372_at	<i>CG5873</i>
8	1623083_at	<i>CG1698</i>
8	1641132_at	<i>CG30497</i>
8	1640494_at	<i>CG13272</i>
8	1639559_at	<i>CG6431</i>
8	1639466_s_at	<i>CG30101</i>
8	1637851_at	<i>CG7422</i>
8	1637562_at	<i>TwdlT</i>
8	1636915_at	<i>CG11380</i>
8	1633217_at	<i>CG30101</i>
8	1630014_at	<i>Nox</i>
8	1629693_at	<i>CG15080</i>
8	1629458_at	<i>CG9411</i>
8	1625293_at	<i>CG14397</i>
8	1625245_at	<i>CG3759</i>
8	1625123_at	<i>CG2962</i>
8	1637830_s_at	<i>CG31145</i>
8	1635127_at	<i>CG34398</i>
8	1634450_a_at	<i>CG14681</i>
8	1632648_at	<i>CG14681</i>
8	1629922_at	<i>CG11409</i>
8	1627752_s_at	<i>SK</i>
8	1626451_at	<i>CG13847</i>
8	1625321_a_at	<i>CG7549</i>
9	1639042_at	<i>CG6414</i>
9	1638481_at	<i>CG2736</i>
9	1637869_at	<i>rdo</i>
9	1636089_at	<i>comm</i>
9	1635199_at	<i>CG6014</i>
9	1633858_at	<i>CG4286</i>
9	1630247_at	<i>CG4554</i>
9	1641413_s_at	<i>CG3074</i>
9	1638277_at	<i>CG11550</i>
9	1636998_at	<i>sca</i>
9	1636835_at	<i>CG16700</i>
9	1632533_at	<i>Timp</i>
9	1631400_at	<i>Cpr66D</i>

9	1628334_at	<i>m4</i>
9	1626910_at	<i>CG15282</i>
9	1626536_at	<i>CG6776</i>
9	1623503_at	<i>sda</i>
9	1639229_at	<i>vkg</i>
9	1625625_at	<i>ImpE1</i>
9	1641476_a_at	<i>Timp</i>
9	1637012_at	<i>m2</i>
9	1629446_at	<i>CG1136</i>
9	1625075_at	<i>Nep2</i>
9	1623950_s_at	<i>Ama</i>
10	1636456_at	<i>CG13053</i>
10	1640342_at	<i>CG6234</i>
10	1640235_at	<i>W</i>
10	1639913_at	<i>Con</i>
10	1636048_at	<i>Dak1</i>
10	1627507_at	<i>CG5704</i>
10	1641535_at	<i>CG9555</i>
10	1639575_at	<i>CG18446</i>
10	1639431_at	<i>synaptogyrin</i>
10	1639152_at	<i>Ptp52F</i>
10	1638810_at	<i>Faa</i>
10	1637495_at	<i>CG18735</i>
10	1636407_at	<i>gol</i>
10	1634597_a_at	<i>CG33970</i>
10	1633869_at	<i>Dfd</i>
10	1632706_at	<i>CG13054</i>
10	1632430_at	<i>Tsf1</i>
10	1630171_at	<i>Cpr97Ea</i>
10	1629914_at	<i>CG34281</i>
10	1629011_at	<i>TwdlN</i>
10	1628779_a_at	<i>svp</i>
10	1626594_s_at	<i>svp</i>
10	1624525_at	<i>CG12998</i>
10	1624403_at	<i>CG13071</i>
10	1636035_at	<i>beat-IIa</i>
10	1630308_at	<i>CG3726</i>
10	1630038_at	<i>pyd3</i>
10	1627511_at	<i>chrb</i>
10	1632082_at	<i>Ndg</i>
10	1640979_at	<i>CG1681</i>
10	1640912_s_at	<i>scarface</i>
10	1639743_s_at	<i>Syn2</i>
10	1637638_s_at	<i>CG10702</i>
10	1634250_at	<i>Act57B</i>
10	1633452_a_at	<i>Rya-r44F</i>
10	1627808_at	<i>CG13011</i>
10	1627515_at	<i>CG10641</i>
10	1623910_at	<i>alphaTub85E</i>
11	1628962_at	<i>CG12708</i>
11	1626641_s_at	<i>glob1</i>
11	1624521_a_at	<i>CG17896</i>
11	1637867_at	<i>mid</i>
11	1635900_at	<i>Thor</i>
11	1641282_at	<i>mthl4</i>
11	1641259_at	<i>Chit</i>
11	1641143_s_at	<i>tsl</i>
11	1638458_at	<i>ImpE1</i>
11	1637658_at	<i>mthl3</i>
11	1636057_at	<i>CG9572</i>
11	1632189_at	<i>CG3587</i>
11	1631498_a_at	<i>fru</i>
11	1627967_a_at	<i>mthl4</i>
11	1626984_at	<i>Gld</i>
11	1624069_at	<i>CG7296</i>
11	1634350_at	<i>sob</i>
11	1633893_at	<i>CG31217</i>
11	1631497_at	<i>Tsp42Eo</i>
11	1626896_at	<i>CG34437</i>
11	1626831_at	<i>CG6579</i>
11	1625950_a_at	<i>CG7777</i>
11	1623197_a_at	<i>zormin</i>
11	1626109_a_at	<i>Drip</i>
12	1641490_s_at	<i>Tsp</i>
12	1640868_at	<i>ato</i>

12	1638961_at	<i>CG14264</i>
12	1638888_at	<i>unpg</i>
12	1637755_at	<i>CG10987</i>
12	1636251_at	<i>Tsp</i>
12	1635562_at	—
12	1634054_at	<i>ninaC</i>
12	1632688_s_at	<i>CG11594</i>
12	1632265_at	—
12	1632226_at	<i>Fie</i>
12	1631665_at	<i>Acp76A</i>
12	1630927_x_at	<i>Pxd</i>
12	1629066_at	<i>GRHRII</i>
12	1628747_at	—
12	1628677_at	<i>Pkcdelta</i>
12	1627979_at	<i>Wnt6</i>
12	1627194_at	<i>I(1)sc</i>
12	1626723_at	<i>Takr86C</i>
12	1625850_at	<i>odd</i>
12	1623959_at	<i>CG1532</i>
12	1623410_at	<i>Pxd</i>
13	1641263_at	<i>CG31816</i>
13	1640057_at	<i>CG9192</i>
13	1639473_at	<i>CG12541</i>
13	1638899_s_at	<i>CG15312</i>
13	1638896_at	<i>Cpr62Bc</i>
13	1638582_at	<i>CG5321</i>
13	1635896_at	—
13	1635835_at	<i>CG30374</i>
13	1635270_at	<i>CG33958</i>
13	1634372_at	<i>Ddr</i>
13	1631774_at	<i>Cpr66Cb</i>
13	1631631_at	<i>Cpr47Ee</i>
13	1631349_s_at	<i>tabor transposon</i>
13	1630142_at	<i>sog</i>
13	1629893_s_at	<i>transposon</i>
13	1629326_s_at	<i>eg</i>
13	1629166_at	<i>sick</i>
13	1627548_at	<i>CG12541</i>
13	1627096_s_at	<i>Tkr</i>
13	1626874_at	<i>Eip63F-1</i>
13	1626133_s_at	<i>transposon</i>
13	1624503_at	<i>CG4786</i>
13	1639694_s_at	<i>Arc1</i>
13	1627734_at	<i>nau</i>
14	1628729_at	<i>vvl</i>
14	1633524_a_at	<i>CalpA</i>
14	1625687_at	<i>kon</i>
14	1633977_at	<i>CG42735</i>
14	1633795_a_at	<i>CG17124</i>
14	1633291_at	<i>dy</i>
14	1631714_a_at	<i>SP71</i>
14	1628993_at	<i>beat-IIb</i>
14	1628301_at	<i>CG32159</i>
14	1625641_s_at	<i>CG9650</i>
14	1624517_at	<i>Ect3</i>
14	1624245_at	<i>CG15239</i>
14	1623601_at	<i>Amyrel</i>
14	1640867_s_at	<i>htl</i>
14	1639605_at	<i>CG33993</i>
14	1639106_at	<i>Grip</i>
14	1636440_at	<i>Sip1</i>
14	1635937_at	<i>CG4500</i>
14	1633387_at	<i>bves</i>
14	1632448_s_at	<i>kel</i>
14	1627478_at	<i>CG33232</i>
14	1626799_a_at	<i>CG16758</i>
14	1625481_a_at	<i>retn</i>
14	1641236_s_at	<i>CG5758</i>
14	1640181_at	<i>CG13044</i>
14	1627499_at	<i>CG2016</i>
14	1624989_s_at	<i>Ef1alpha100E</i>
14	1624982_s_at	<i>CG5080</i>
14	1638132_at	<i>CG10184</i>
15	1635768_at	<i>CG4670</i>
15	1634842_a_at	<i>CG11160</i>

15	1633262_s_at	<i>Lim1</i>
15	1626806_at	<i>tra</i>
15	1626059_at	<i>knrl</i>
15	1625620_a_at	<i>Sxl</i>
15	1640139_at	<i>B-H2</i>
15	1639797_at	<i>CG34109</i>
15	1636203_at	<i>B-H1</i>
15	1632868_a_at	<i>wg</i>
15	1631115_at	<i>Obp8a</i>
15	1629733_at	<i>Lim1</i>
15	1629612_at	<i>CG31158</i>
15	1629333_at	<i>CG32683</i>
15	1626665_at	<i>CG7408</i>
15	1626150_at	<i>tsh</i>
15	1625671_at	<i>lectin-37Db</i>
15	1625220_at	—
15	1625145_a_at	<i>Anxb11</i>
15	1629097_at	<i>kni</i>
15	1624060_at	<i>bab2</i>
15	1638037_a_at	<i>dpr17</i>
15	1625207_at	<i>CG32636</i>
15	1623006_at	<i>SerT</i>
15	1623466_at	<i>bab1</i>
16	1641068_a_at	<i>spz</i>
16	1640607_at	<i>org-1</i>
16	1639545_a_at	<i>Awh</i>
16	1635987_at	<i>CG12116</i>
16	1635886_s_at	<i>blood transposon</i>
16	1633264_at	<i>CG13024</i>
16	1630969_s_at	<i>CG12206</i>
16	1641648_at	<i>CG3939</i>
16	1639541_at	—
16	1639353_at	<i>CG17032</i>
16	1637803_s_at	—
16	1633396_at	<i>btd</i>
16	1632372_at	<i>CG31076</i>
16	1631867_at	<i>ldgf5</i>
16	1630608_at	<i>CG14608</i>
16	1627071_at	<i>dpr</i>
16	1626058_at	<i>lbl</i>
16	1636387_at	<i>CG10300</i>
16	1632019_s_at	<i>CG9008</i>
16	1628878_at	<i>al</i>
16	1624942_at	<i>bab1</i>
16	1624819_s_at	<i>gypsy transposon</i>
16	1630120_s_at	—
16	1639333_at	<i>al</i>
16	1637813_at	<i>abd-A</i>
16	1636558_a_at	<i>abd-A</i>
16	1633383_at	<i>toe</i>
16	1633299_at	<i>lz</i>
16	1632742_at	<i>eyg</i>
16	1631783_at	<i>CG4267</i>
16	1624802_at	<i>CG31686</i>
16	1623776_s_at	<i>dsx</i>

*Cluster number as displayed in Fig. 2B.

[†]Affymetrix probe set ID.

[‡]Annotated gene corresponding to probe set [if blank (—), the probe set maps to an unannotated region of the genome].

Table S6. Mean number of matches to the consensus Dsx binding sequence per significant and non-significant gene

Category	Distance from gene*				
	≤500 bp	≤1000 bp	≤2000 bp	≤5000 bp	≤10,000 bp
L3					
Significant	2.18	2.24	2.38	2.76	3.60
Non-significant	0.79	0.85	1.01	1.58	2.68
P-value [†]	1.23×10^{-7}	2.55×10^{-6}	6.01×10^{-5}	1.16×10^{-2}	2.53×10^{-2}
P6					
Significant	1.21	1.28	1.48	2.04	3.02
Non-significant	0.78	0.85	1.01	1.58	2.68
P-value	1.11×10^{-8}	2.38×10^{-8}	3.30×10^{-8}	1.35×10^{-5}	1.09×10^{-2}
P20					
Significant	1.15	1.22	1.46	2.07	3.20
Non-significant	0.78	0.85	1.00	1.57	2.67
P-value	6.34×10^{-4}	4.02×10^{-4}	4.06×10^{-6}	1.30×10^{-5}	2.36×10^{-4}
ALL[‡]					
Significant	1.16	1.24	1.45	2.03	3.09
Non-significant	0.78	0.84	1.00	1.57	2.67
P-value	7.58×10^{-9}	7.20×10^{-9}	1.74×10^{-10}	2.49×10^{-8}	9.83×10^{-5}

*Only non-coding sequences are considered. If a match to the consensus Dsx binding sequence lies between the start and end of a gene (as annotated in FlyBase R5.29), its distance is recorded as 0 bp. Otherwise, its distance is recorded as the number of bp between it and the start of the gene.

[†]The P-value is based on a two-sided Wilcoxon rank sum test of the hypothesis that the number of matches is the same for 'significant' (differentially expressed at FDR threshold of 0.05) and 'non-significant' (not differentially expressed at FDR threshold of 0.05) genes.

[‡]For the category 'ALL', 'significant' genes are those that are differentially expressed at FDR threshold of 0.05 at at least one developmental stage.

Table S7. Mean density of matches to consensus Dsx binding sequence per significant and non-significant gene

Category	Distance from gene*				
	≤500 bp	≤1000 bp	≤2000 bp	≤5000 bp	≤10,000 bp
L3					
Significant	0.131	0.125	0.123	0.122	0.128
Non-significant	0.097	0.102	0.106	0.112	0.117
P-value [†]	1.14×10 ⁻⁴	3.66×10 ⁻³	1.08×10 ⁻¹	5.11×10 ⁻¹	3.39×10 ⁻¹
P6					
Significant	0.107	0.110	0.122	0.126	0.123
Non-significant	0.097	0.102	0.106	0.112	0.117
P-value	8.12×10 ⁻⁵	5.85×10 ⁻⁴	2.03×10 ⁻³	3.32×10 ⁻²	3.83×10 ⁻¹
P20					
Significant	0.099	0.109	0.126	0.130	0.132
Non-significant	0.097	0.102	0.106	0.111	0.116
P-value	1.94×10 ⁻²	1.47×10 ⁻²	2.20×10 ⁻³	9.48×10 ⁻⁴	3.57×10 ⁻³
ALL[‡]					
Significant	0.100	0.107	0.121	0.126	0.127
Non-significant	0.097	0.101	0.106	0.111	0.116
P-value	1.07×10 ⁻⁴	3.04×10 ⁻⁴	3.45×10 ⁻⁴	1.20×10 ⁻³	2.57×10 ⁻²

*Only non-coding sequences are considered. If a match to the consensus Dsx binding sequence lies between the start and end of a gene (as annotated in FlyBase R5.29), its distance is recorded as 0 bp. Otherwise, its distance is recorded as the number of bp between it and the start of the gene. The density is calculated as the number of matches divided by the length (in kb) of the considered region for each gene. This length is the sum of the upstream length (which is equal to the window size of 0.5, 1, 2, 5 or 10 kb) and the downstream length (which is equal to whichever is the greater of the window size or the length of the gene).

[†]The P-value is based on a two-sided Wilcoxon rank sum test of the hypothesis that the density of matches is the same for 'significant' (differentially expressed at FDR threshold of 0.05) and 'non-significant' (not differentially expressed at FDR threshold of 0.05) genes.

[‡]For the category 'ALL', 'significant' genes are those that are differentially expressed at FDR threshold of 0.05 at at least one developmental stage.